SEMMELWEIS EGYETEM

DOKTORI ISKOLA

Ph.D. értekezések

3389.

SCHNEIDER BENCE

Magatartástudományok

című program

Programvezető: Dr. Kovács József, egyetemi tanár

Témavezető: Dr. Bódizs Róbert, tudományos főmunkatárs

The spectral slope of the EEG as an indicator of sleep depth and architecture

PhD thesis

Bence Schneider

Semmelweis University Doctoral College
Mental Health Sciences Division

Supervisor:
Róbert Bódizs, Ph.D.

Official reviewers:
Máté Baradits, M.D., Ph.D.
Zoltán Bálint, Ph.D.

Head of the Complex Examination Committee:
Ágnes Lukács, Ph.D.

Members of the Complex Examination Committee:
Gábor Csukly, M.D., Ph.D.
Ágnes Szöllősi, Ph.D.

Budapest
2025

Contents

List of abbreviations

ADHD	Attention-deficit hyperactivity disorder
ANOVA	Analysis of variance
ANCOVA	Analysis of covariance
BOLD	Blood oxygenation level dependent
EEG	Electroencephalography
FFT	Fast Fourier Transform
ECoG	Electrocorticography
fMRI	Functional magnetic resonance imaging
FOOOF	Fitting of oscillations & one over f
HC	Healthy controls
IRASA	Irregular resampling auto-spectral analysis
LFP	Local field potential
NREM	Non-rapid eye movement
MDD	Major depressive disorder
MEG	Magnetoencephalography
PSD	Power-spectral density
REM	Rapid eye movement
SWA	Slow wave activity
SWS	Slow wave sleep
TST	Total sleep time
WASO	Wake after sleep onset

1 Introduction

Since the invention of electroencephalography and the first observations made by Hans Berger, through modern classics like *Rhythms of the Brain* (Buzsáki, 2006), oscillations have been in the foreground of the study of electric brain activity. Yet neural activity comprises an ever-present stochastic, wide-band component in the background of discrete oscillations, observable on multiple scales, from fluctuations of membrane potentials to the scalp EEG, which had been termed as *background activity* or *neural noise*. However, recently there is a rapidly growing interest in this background component, as evidence accumulated that it carries physiologically meaningful information, spanning a set of not completely equivalent, but overlapping terminologies like *scale-free*, *fractal*, *aperiodic* or *1/f* neural activity. (Making a quick search on PubMed, National Library of Medicine on articles that include one of the above terms in their title or abstract together with the term "EEG", 1002 results were found, more than half of which have been published in the last 5 years.)

Despite the differences in naming, a uniting feature is the power-law spectra of the signals, more precisely a relationship between the power-spectral density (PSD) P and frequency f such that:

$$P(f) = c \cdot f^x$$

where x is the spectral exponent, which in this context usually takes a negative value, as spectral power decays with increasing frequency. Transforming both axes to the log-domain, we can get a linear relationship:

$$\ln[P(f)] = \ln(c) + x \cdot \ln(f)$$

where x is the spectral slope and $C := \ln(c)$ is the spectral intercept.

1.1 Power-law spectra in neural signals

One of the earliest studies regarding the log-log spectra of the EEG (Matthis et al., 1981) considered the spectral slope as a potential indicator of cerebral changes in a child with brain stem tumor, another analysis (Feinberg et al., 1984) already observed the linear relationship between log amplitude and log frequency, stating effects of aging on the spectral slope in NREM sleep, namely the slope flattening in the older population. Still in an early study, the removal of the power-law trend of the spectrum had been proposed as a preparation step in the analysis of oscillations (Dumermuth and Molinari, 1987, Sörnmo and Laguna, 2005). In Pritchard, 1992 the

spectral slope of resting state EEG of 10 healthy adults was systematically analyzed, revealing effects of topography on the spectral exponent. Furthermore, the lack of a characteristic time-scale of the EEG background was pointed out, identifying the signal as a fractal with respect to time.

Power-law spectra were identified also in subdural ECoG recordings in the high frequency range of $80 - 500\ Hz$, with the exponent of -4 being stable between subjects, brain region and local neural activity level (Miller et al., 2009). A crossover was detected in the spectra at around $75Hz$ indicating the presence of multiple time-scales in brain activity, below this frequency the exponent of -2.5 was fitted.

Task-related modulations and regional variations in the aperiodic activity were found in ECoG recordings (He et al., 2010). In order to test the functional significance of scale-free activity, a visual cue detection task was performed, which revealed spectral slope differences between rest and different task types in multiple recording locations, in each case spectra became flatter during task performance. Locations where significant differences were found included the primary motor cortex of the hand, Broca's area, lateral occipital cortex and lateral temporal lobe. Resting state fMRI BOLD signals also show power-law spectra and region specific, regional differences were observed for the spectral exponents, with steepest spectra in the visual regions and the default network, and flattest spectra in the cerebellum and hippocampus.

Flattening of the spectrum was observed with aging and with increasing task difficulty as well. In addition the slope of the $1/f$ neural noise mediated age-related visual working memory decline, and flatter spectra was associated with longer reaction times in a visual working memory task (Voytek et al., 2015).

The spectral slope has also proved to be sensitive to different disorders. It was shown that children with attention-deficit/hyperactivity disorder (ADHD) show significantly steeper EEG power-spectra compared to typically developing children, and that after medication these effects disappear, suggesting that the spectral slope also reflects atypical brain activity present due to the disorder (Robertson et al., 2019). Another study proposed that the aperiodic component of the power spectrum is a better marker of schizophrenia, than the traditionally used power-bands or task-based assessment, which is a major finding, as behavioral measurements are the standard in the clinical setting (Peterson et al., 2023).

1.1.1 Possible sources of scale-free activity in the brain

The scale-invariant property of power-spectral distributions in the EEG also raised the question, whether it is a sign of criticality, as $1/f$ noises commonly appear

in complex systems near a critical point. Here multiple aspects of neural activity support the hypothesis, as EEG, MEG, ECoG and LFP spectra all exhibit scale-free properties, furthermore the avalanche-like propagation of firing in in-vitro neuronal populations exhibited power-law distributions in multiple regards, like avalanche size, duration. In addition, the power-law like distributions of the neural activity appeared to be an inherent property, as the system arrived into the state without any external input, thus the hypothesis of self-organized criticality had been proposed. In this view, brain organization and activity is self-tuned to a critical point that has optimizes properties like information propagation and network stability, which were also demonstrated in simulated neuronal networks (Beggs and Plenz, 2003).

Spectral slope differences were found between sleep and awake states in LFP recordings in cats, with steeper slopes in slow wave sleep than in wake, however, it was also pointed out that power-law like spectra do not necessarily imply criticality, and some evidence against the theory was also put forward, namely inter-spike-interval distributions recorded in the cat parietal cortex didn't exhibit long term correlations, and avalanche distributions were not confirmed in-vivo in this case (Bédard et al., 2006).

Another mechanism that could generate power-law spectra in the ECoG signals was suggested in Freeman and Zhai, 2008, by the simulation of mutually excited pyramidal cells in the cortex, accurately modeling changes in the spectral slope of the ECoG in wakefulness and sleep. Here the response of a neuron to a unit impulse was modeled by the summation of two exponential processes, a rapidly rising and a slower decaying function, which was then convolved with a Poisson point process, creating a signal similar to the ECoG in the frequency domain. The spectral slope of the simulated signals is dependent on the rise-time of the exponential term in the response function of the neuron. They theorize that the homeostatic regulation of refractory times of excitatory neurons is the explanation for the variation in the spectral slopes.

A similar modeling approach was presented by Gao et al., 2017 proposing that alterations in the spectral slope reflects changes in the excitation/inhibition (E/I) balance of neural circuits. The sum of exponentials model was used, as before, to represent the response of individual neurons, with the difference that two types of neuron populations were defined. Excitatory neurons had shorter rise and decay times, while inhibitory neurons rose and decayed more slowly, but the response was of the opposite sign. The total excitatory and inhibitory currents were calculated as the convolution of a Poisson process with these response functions, finally summed to create the simulated LFP series. As the rise times were different for the excitatory

and inhibitory currents, the spectral slope were different as well (steeper for the inhibitory). As the balance between the contributions of the two currents was varied, representing the alteration of excitation and inhibition ratio, a change was reflected in the spectral slope of the total simulated LFP. The hypothesis that a link between micro and macro scale phenomena has been made seems intriguing, however, the E/I ratio had been significantly correlated with the spectral slope only in the 30-50 Hz range, while empirical measurements show much power-law like spectra in a much wider band.

In another attempt (Milstein et al., 2009) to explain the $1/f$ scaling of LFP power spectra, a shot noise model was adopted, known from the field of electronics, more precisely in the noise in an electric resistors, first described by Schottky. In an analytical model, the loose assumptions were made that each neuron has its own stereotypic extracellular contribution profile to the total potential, and that this specific profile is repeated by each neuron according to a point process that corresponds to its spike train. In addition, it was required that the system is in a stationary state, so that its autocorrelation is independent of time and, as observed in practice, that the power-spectrum respects a power-law. Two solutions were proposed for the problem, first, that the extracellular field of neurons are characterized by a much slower decay time than rise time, thus given a Poisson-like spike train of independent activations, the PSD of the local field could have the observed shape of $P(f) \propto f^{-2}$, similar to Brownian noise. The second possibility was that the extracellular field of the neuron is has the shape of a sharp peak, and the point process of the spike train is not a simple Poisson process, more exactly the spike timing correlations are linear. Such a process is the so-called telegraph process, which consists of periods of sustained rapid activity, followed by intervals of inactivity, which can be similar to the alternation of UP-DOWN states in the cortex.

1.1.2 The spectral slope reflects arousal level and sleep stages

Among other non-linear parameters, the sleep stage specificity of the EEG spectral exponent had been observed, with flattest spectral slopes in wake ($x \approx -1.5$) and steepest in slow-wave sleep ($x \approx -3$) (Pereda et al., 1998). Consistent with differences found in ECoG data between awake and slow wave sleep states (Zempel et al., 2012). Chemically induced alterations in arousal was also pointed out, as the effects of certain anesthetics produced significantly steeper spectra. The steepening of the spectral slope coincided with the loss of consciousness, which was the case for propofol and xenon, but not for ketamine, where both the wake-like spectral slope and conscious experiences persisted (Colombo et al., 2019). The spectral slope was

proposed as an accurate marker of arousal levels (Lendner et al., 2020), as it did not only delineate between wake from deep sleep and states of anesthesia, but also REM sleep, which in other aspects had more wake-like features. Age-specific changes in sleep are also reflected in the spectral exponent, as sleep depth deteriorates with the progression of age, EEG spectra become flatter in NREM sleep (Bódizs et al., 2021b, Bódizs et al., 2024), see Figure 1A. Changes in successive sleep cycles in the spectral slope show a flattening over the course of the night, also suggesting that the aperiodic component reflects accumulated sleep pressure (G. Horváth et al., 2022).

Shallower EEG spectra in N2 and N3 were found characteristic of insomnia and sleep state misperception (Bódizs et al., 2024), possibly explained by increased high frequency activity present in insomnia. When comparing pooled overnight spectral slopes from a control group and insomnia patients (11 participants for each group), a bimodal distribution could be noticed. In the control group the dominant mode of the spectral slope distribution was below -2, corresponding to sleep, while in the insomnia group this peak was diminished and values above -2 and closer to -1 were most frequent, see Figure 1C. Patients with NREM parasomnias (sleepwalking, sleep-related eating disorder, confusional arousals or sleep terrors) were characterized by steeper spectral slopes than patients with sleep-related hypermotor epilepsy in N3 sleep stage, which is a significant finding, as the differential diagnosis of the two has been a challenging task for sleep physicians and epileptologists (Pani et al., 2021).

We showed that the spectral slope of the EEG is different for sleep stages (Schneider et al., 2022) and reflects sleep homeostasis in general, as it showed clear rebound effects after accumulated sleep pressure during a sleep deprivation experiment (G. Horváth and Bódizs, 2025, Bódizs et al., 2024).

1.2 Methods for separating the oscillatory and aperiodic components

In the following we present two methods that aim to separate the oscillatory and aperiodic components in time-series, which can be useful for two reasons. First, the broadband aperiodic neural activity can be studied, parameters like the spectral slope, intercept or knee extracted. Second, after removing the aperiodic background, or 'whitening' the spectra, oscillations will not be confounded with changes in background activity offset of rotation, a pitfall that traditional frequency band-based methods do not avoid (Donoghue, Dominguez, and Voytek, 2020).

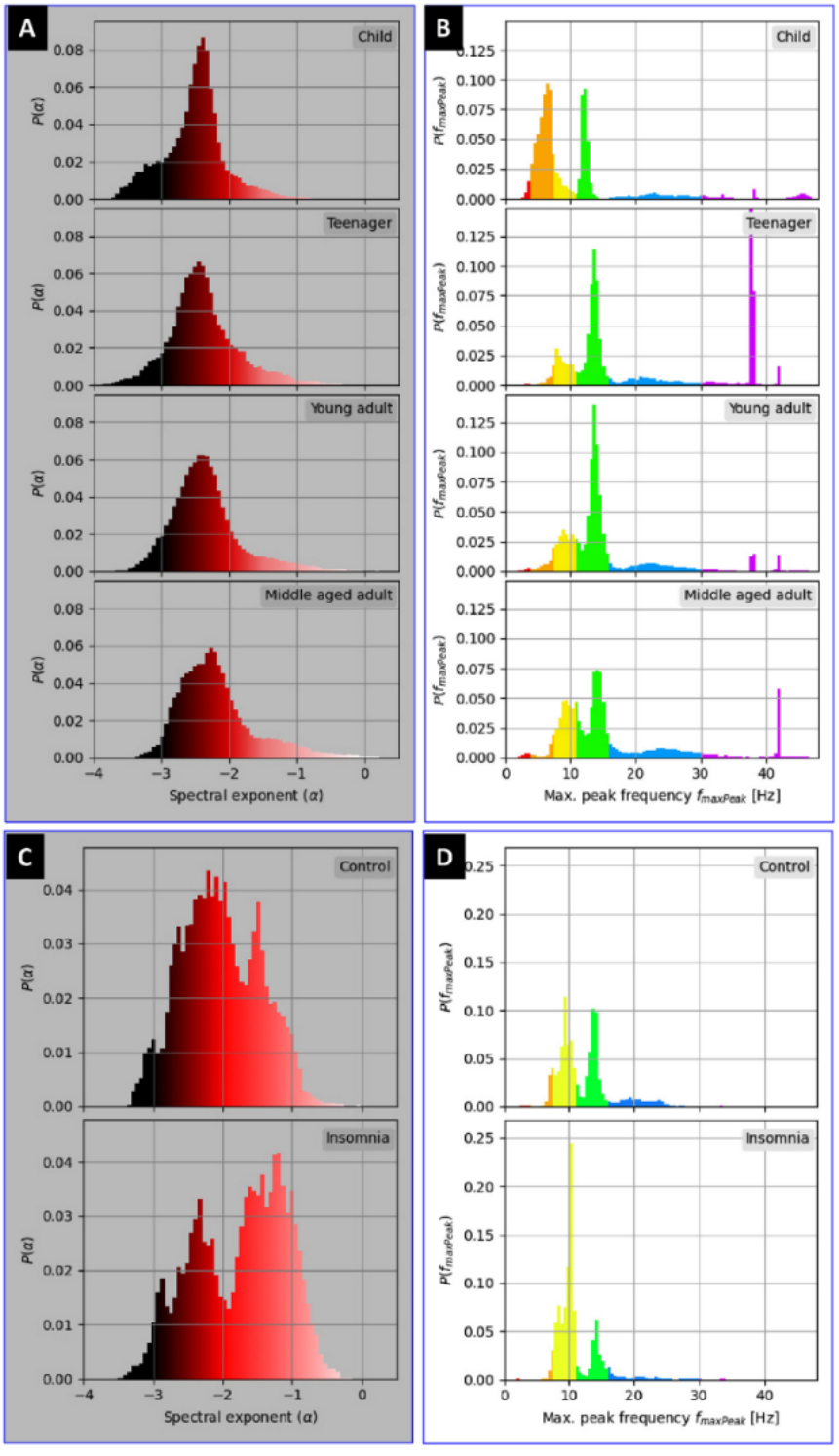

Figure 1: Effects of aging and insomnia on the spectral parameters: A) distribution of spectral slopes per age group, B) distribution of spectral peak frequencies per age group in the Budapest-München database of 251 healthy subjects. Correspondingly, C) distribution of spectral slopes and D) peak frequencies in insomnia patients vs. control group, 11 subjects per group. (Adopted with permission from Bódizs et al., 2024)

1.2.1 FOOOF

Probably the most popular algorithm for the parametrization of neural spectra is the *Fitting oscillations & one over f* (FOOOF) method (Donoghue, Haller, et al., 2020, recently renamed to Specparam). It is a physiologically informed model of the power spectrum that can be fitted to different electrophyisiological signals including EEG, MEG, ECoG and LFP.

The model is based on the assumption that neural activity is composed of two distinct functional processes:

- An aperiodic background, reflected in the spectrum as a decaying power-law
- A variable number of oscillations, represented by gaussian peaks in the power-spectrum.

Mathematically the FOOOF model (Eq. 1) describes the observed power-spectra as the sum of the an aperiodic $[L(f)]$ and oscillatory $[G(f)]$ component in the $\log_{10}$ power domain. The aperiodic component is defined as a power-law defined by the spectral exponent (x) and intercept (b), optionally a knee (k) parameter that defines a frequency under which the aperiodic component flattens to a slope of 0, see Equation 2. The oscillatory component is a sum of a custom number of Gaussian functions (G_n), each described by a peak amplitude (a), peak center frequency (f_c) and peak bandwidth (w), Equation 3.

$$\log_{10}[P(f)] = L(f) + \sum_{n} G(f)_n \tag{1}$$

$$L(f) = b - log_{10}(k + f^x) \tag{2}$$

$$G(f)_n = a \cdot exp(\frac{-(f - f_c)^2}{2w}) \tag{3}$$

The FOOOF method iteratively approximates the aperiodic and oscillatory components, by first fitting a power-law, which is subtracted from the original spectrum to achieve a whitened PSD. The whitened version is fitted with multiple Gaussians, until no peaks are found above a predefined peak threshold, establishing the oscillatory component. Next, the oscillatory component is subtracted from the original PSD to remove the spectral peaks and the aperiodic component fitted again. Finally, the oscillatory components are added to the last aperiodic fit resulting in the final model.

1.2.2 IRASA

Another well-known method is the *Irregular-Resampling Auto-Spectral Analysis* (IRASA, Wen and Liu, 2016) which also aims to separate the fractal and oscillatory components, with one of the differences being that it utilizes the time-domain signals as its input, not the pre-calculated power-spectra.

Given the time domain signal $y(t)$, the method aims to separate the fractal $f(t)$ and $x(t)$ oscillatory processes, that are part of the additive model:

$$y(t) = f(t) + x(t)$$

Assuming that $f(t)$ is a fractal in the time-domain, the self-affine property of fractals can be used, stating that after resampling a fractal series $f(t)$ by a factor of h, the statistical properties of the new signal $f_h(t)$ is the same as that of the original scaled by the factor of h^H, (where H is the Hurst exponent) (Mandelbrot and Van Ness, 1968). In the frequency domain this means that the resampled time-series has the same amplitude spectrum as the original one, only rescaled by h^H:

$$F_h(\omega) = h^H \cdot F(\omega)$$

where $F(\omega)$ and $F_h(\omega)$ are the amplitude components at specific frequencies ω of the Fourier transform of time-domain signals $f(t)$ and $f_h(t)$ respectively. The above rescaling holds in the frequency domain only if $F(\omega)$ takes the form of a power-law. In contrast the resampling of the oscillatory component that is non-zero only at sparse number of frequencies causes a frequency shift in the amplitude and power spectra. Based on the above assumptions and properties, an estimate of the fractal power-spectrum $F^2(\omega)$ can be made by taking the median of multiple rescaled versions of the geometric means $\bar{S}_h(\omega)$ calculated from up- and down-sampled observed spectra by factor pairs of h and $1/h$:

$$\bar{S}_h(\omega) = \sqrt{S_{y_h y_h}(\omega) \cdot S_{y_{1/h} y_{1/h}}(\omega)}$$

$$F^2(\omega) = median_h\{\bar{S}_h(\omega)\}$$

In order to irregularly resample the signals, the scaling factors of $0.9 \leq h \leq 1.1$ are used with a step of 0.05, ensuring that possible harmonics of the oscillatory component do not overlap after the resampling, and get eliminated in the fractal spectrum estimate.

2 Objectives

Based on observations that in addition to neural oscillations, the electric activity of the brain includes an aperiodic, fractal background component, which reflects meaningful information about states of arousal and consciousness, we adopted a model of the EEG frequency spectrum that captures the aperiodic component using a power-law linking the frequency and power spectral density, then assessed how parameters of this model reflected different aspects of sleep.

First, we aimed to assess the effects of sleep stage, sex, age and brain region on the spectral parameters of the EEG during sleep in a healthy population, in search of mathematically well-defined markers of objective sleep depth.

Second, to provide an algorithm for sleep cycle detection utilizing the overnight dynamics of the spectral slope, and compare the newly defined cycles to classical, manually annotated ones. Besides testing the cycle detection algorithm on a healthy sample, sleep data from major depression disorder patients was included in our analysis, in an attempt to test our method's sensitivity to alterations in sleep structure present due to the disorder and different types of antidepressant medications.

Overall, the objectives of our work had been to explore the behavior of fractal parameters during sleep in more detail, and at the same time to lay the foundations of a more objective, quantitative methodology of sleep depth and structure measurement, alternative to time-consuming and potentially subjective sleep staging and cycle annotation.

3 Methods

3.1 Study 1 - Scale-free and oscillatory spectral measures of sleep stages in humans

3.1.1 Materials and Equipment

In the study Schneider et al., 2022, EEG recordings from the Budapest-Münich polysomnographic database were used that included 251 healthy subjects (122 females) from a wide age range (4-69 years). Age groups were adopted as defined in a previous study (Bódizs et al., 2022): children (4–10 years, N = 31), teenagers (10–20 years, N = 36), young adults (20–40 years, N = 150), and middle-aged adults (40–69 years, N = 34). Ten EEG channels (Fp1, Fp2, F3, F4, P3, P4, C3, C4, O1, O2; see Figure 2) were analysed with placements according to the 10-20 standard (Bódizs et al., 2022).

The database is a result of a multi-laboratory study, as such, some technical parameters of the EEG recording equipment differed (precision, sampling rate, filter settings), however they all captured a whole night of undisturbed sleep after an adaptation night. The adaptation nights were part of the procedure to decrease possible first-night effects on sleep, and not included in the database. In order to eliminate differences in the recording hardware, the amplitude reduction of the EEG amplifiers were measured in the 0.05-100 Hz frequency range and used to correct the power-spectral densities (see Materials and Methods in Ujma et al., 2017). The recordings were mathematically re-referenced to a linked-mastoid setup before processing. Hypnograms were available from the database as recordings were previously scored according to the American Academy of Sleep Medicine (AASM) rules (Berry et al., 2018), however a $20s$ epoch length was employed from the Rechtschaffen & Kales methodology (Rechtschaffen A, 1968), furthermore visual annotations of artifacts were also at our disposition with a higher, $4s$ resolution.

3.1.2 Power spectrum calculation

The power-spectral densities (PSDs) were calculated for each sleep stage, subject and electrode. The signals were segmented into windows of $4s$ length with $2s$ overlap, windows that contained any artifacts were excluded, than a Hanning-window was applied, and the squared absolute values of the FFT evaluated. As the window length was fixed (and the NFFT sample numbers equal to 4 times the sampling frequency), a common frequency resolution of 0.25 Hz was achieved in the PSDs, irrespective of differences in original sampling rates. Average PSDs for each subject,

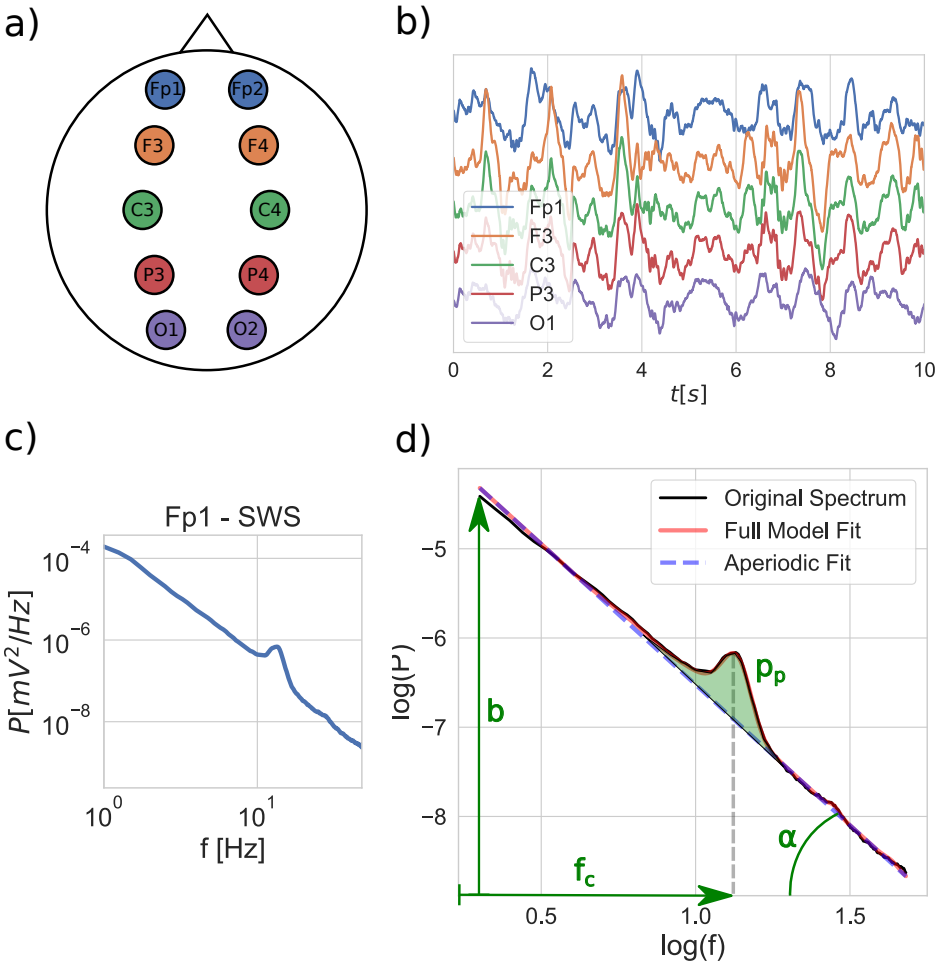

Figure 2: Schematic outline of the fitting process: **a)** EEG is recorded with electrodes placed according to the 10–20 system, out of which 10 are used, covering 5 brain regions on both left and right hemispheres. **b)** Time domain signals are segmented into 20 s windows and grouped by sleep stages for each EEG channel. **c)** Average power-spectral density is calculated for each sleep stage per channel. **d)** The FOOOF model is fitted to the average power spectra, and the model parameters are extracted: spectral slope [$x = tan(\alpha)$], intercept (b), peak central frequency (f_c), and peak power (p_p). (From Schneider et al., 2022 with permission.)

electrode and sleep stage were created using Welch's method.

3.1.3 Model fitting

The spectral slope and intercept along with spectral peaks parameters were extracted from each PSD using the "Fitting of Oscillations and One Over F" (FOOOF) method (Donoghue, Haller, et al., 2020).

The fitting was applied to the 2-48 Hz frequency range, resulting good fits in general (with R^2 coefficients of determination min.:0.6401, mean: 0.9908, max.:0.9999). The range was chosen as it is the widest stable region of the power-law in the spectrum during sleep. Part of the EEG signals were hardware filtered at 0.5 Hz, thus low frequency oscillations $< 1Hz$ could not always be fully resolved, which could be confused with aperiodic activity by the FOOOF fitting method, a common challenge of current methods, also discussed in the literature (Gerster et al., 2022). The upper boundary of 48 Hz was chosen in order to avoid the 50 Hz power line peak, and regardless, no significant scalp EEG activity is expected above this frequency during sleep. Some parameters of the method were altered in order to avoid over- and underfitting, to get a better resolution of spectral peaks the peak bandwidth range was set to 0.7-4 Hz and the peak threshold to 1.

3.1.4 Statistical analysis

The parameters included in the statistical analyses were: the spectral slope, center frequency and power of the dominant peak. Assessing the relationship between the spectral slope and intercept, a strong correlation was revealed. To eliminate this dependence an alternative definition of the intercept was used, namely the power of the aperiodic component at the frequency of the dominant peak, as it was pointed out before, this is the frequency location at which the aperiodic power shows the least correlation with the spectral slope (Bódizs et al., 2021a).

Considering each spectral parameter as the dependent variable, general linear model analysis (repeated measures ANOVA with sigma restricted parametrization) was carried out while considering factors of sex and age group, and within-subject effects of sleep stage: WAKE, NREM1, NREM2, SWS, REM (corresponding AASM stage codes: W, N1, N2, N3, R), brain region (frontopolar, frontal, central, parietal, occipital) and laterality (left, right).

3.2 Study 2 - Fractal cycles of sleep, a new aperiodic activity-based definition of sleep cycles

In **Study 2** (Rosenblum, Jafarzadeh Esfahani, et al., 2025) a novel sleep cycle detection method had been introduced, based on the overnight dynamics of the spectral slope of the fractal EEG component. The newly defined 'fractal cycles' were compared to classical, manually annotated sleep cycles, assessing correlations of cycle durations between the two methods, as well as the detection of skipped REM stages in a population of healthy subjects and a group of patients with major depressive disorder (MDD).

3.2.1 Materials

A total of 337 polysomnographic recordings were used to compare the two methods, combined from six datasets, that included 205 healthy adults from a wide age range of 18-75 years (mean: 36.7 ± 15.0 years), 118 females (Datasets 1-5) and 21 healthy children and adolescents between the ages of 8 and 17 years (mean: 12.4 ± 3.1 years), (Dataset 6). Datasets 1-3 also included 111 patients with MDD. Out of the six datasets five were recorded in a sleep laboratory (Dataset 1,2,3,5,6) and one at the participants' home (Dataset 4) using polysomnographic devices, for more detailed information about the datasets and recording devices see Table 1. EEG electrodes F3 and F4 were used as these were common in all datasets except one (in Dataset 1 channel C3 and C4 were analysed in lack of frontal electrodes).

	Dataset 1	Dataset 2	Dataset 3	Dataset 4	Dataset 5	Dataset 6
Original study	Rosenblum et al., 2023			Jafarzadeh Esfahani et al., 2023	Rosenblum et al., 2024	Furrer, 2019 Volk, 2019 Jaramillo, 2020
Healthy participants	38	39	33	34	62	21
MDD patients	40	38	33	0	0	0
Recording environment	Lab	Lab	Lab	Home	Lab	Lab
Nr. of channels	4	128	32	24	16	128
Sampling rate [Hz]	250	200	250	256	250	500
Analyzed electrodes	C3, C4	F3, F4	F3, F4	F3, F4	F3, F4	F3, F4
Epoch length [s]	30	30	30	30	30	20

Table 1: Specifications of the datasets used in the analysis. (Adapted from Rosenblum, Jafarzadeh Esfahani, et al., 2025.)

3.2.2 Classical definition of sleep cycles

Given the hypnograms from two independent scorers, the classical cycles were established manually based on the original definition of sleep cycles (Feinberg and Floyd, 1979), and some minor alterations. The beginning of a cycle could be N1, N2, in

some cases wake, succeeded by at least 20 min of N2 or slow-wave (SWS) sleep, finally, the cycle is terminated at the following REM stage's end, with possible short interruptions by wake or NREM sleep. In a few instances, the cycle end was set to a NREM or wake stage. The last cycles toward the end of the night not terminated by REM were removed if shorter than 50 minutes, kept otherwise.

Cycles with skipped REM stages at the end and with longer durations than 110 minutes were manually split into two cycles during visual inspection and flagged 'skipped' if:

- The cycle contained lightening of sleep (wake, N1 or N2) in the middle instead of REM.
- There was a period of uninterrupted wake, N1, N2 or movement longer than 12 minutes preceded and succeeded by SWS.
- If lighter sleep (or wake) clearly separated two episodes of SWS.

3.2.3 Fractal activity-based cycles of sleep

The proposed method, 'fractal cycles' for short, aims to give an objective, automatically computable definition of sleep cycles based on the fractal (or aperiodic) activity of the brain, more precisely the local extrema in the overnight dynamics of the spectral slope of the electroencephalogram.

The offline analysis of the EEG signals was executed with MATLAB (vR2021b), using the Fieldtrip toolbox and custom scripts. After averaging the time domain signals of the two electrodes, F3 and F4, (C3 and C4 in the case of Dataset 1), the power spectra were calculated for each epoch and the fractal component separated from the oscillatory spectral component using the Irregular-Resampling Auto-Spectral Analysis (IRASA) method (Wen and Liu, 2016). The spectral slopes were then calculated in the log-log domain, using the *logfit* function in the $0.3 - 30$ Hz frequency range. The 0.3–30 Hz and 30–48 Hz region was considered separately, the latter didn't distinguish sleep stages as consistently, so the 0.3-30 Hz was adopted for cycle detection. Another comparison was made with the 1-30 Hz range as well, however after applying the Savitzky-Golay filtering it yielded the same slope time series as the 0.3-30 Hz band. We would like to note that the spectral slopes calculated in the two studies are comparable despite the differences in the fitting method and range. Assuming that he power-law spectra underline a scale independence between frequency and power, the spectral slope is not expected to be dependent on the fitting range in general, so this might be considered a technical detail.

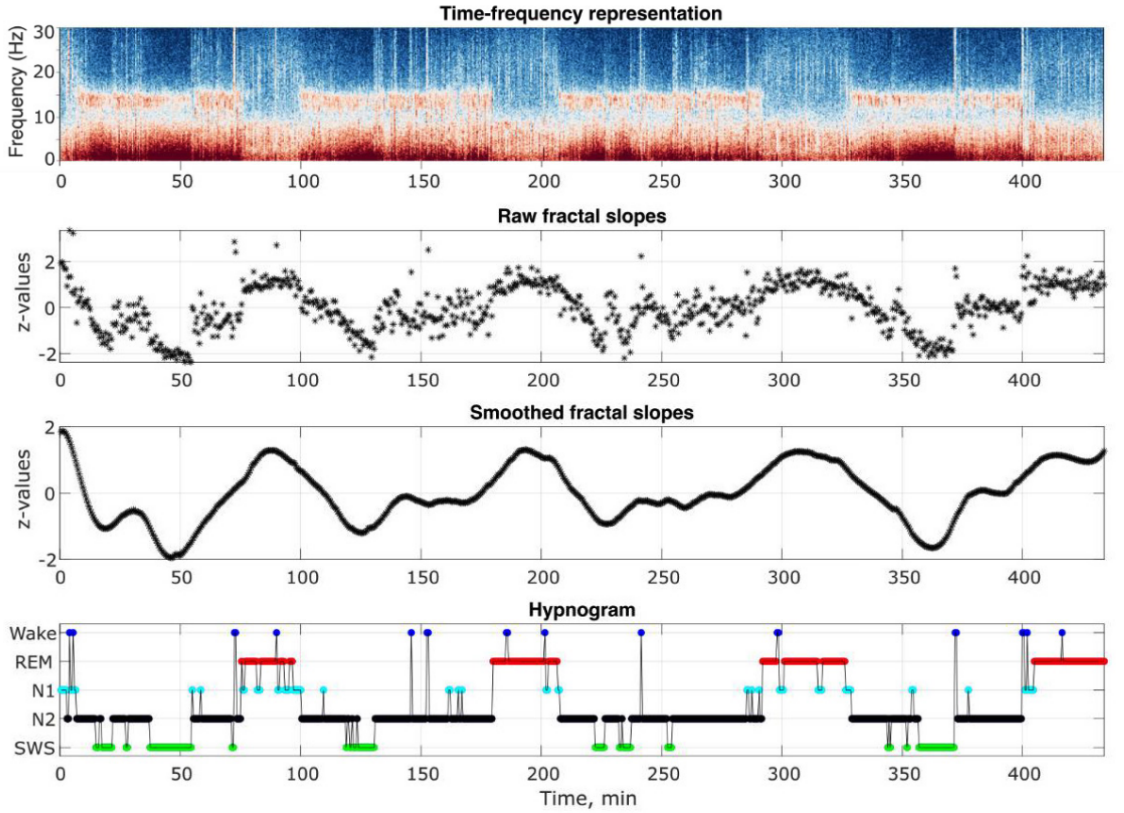

Figure 3: Steps of the 'fractal cycles' method: spectral slopes are calculated from the power spectral data for each epoch, then smoothed and z-normalized. The fractal cycles are defined as the interval between two consecutive local maxima that exceed the amplitude of 0.9 z and are at least 20 minutes apart. As local minima correspond to deeper stages of sleep and local maxima are reached during REM or lighter sleep, the cyclic nature and correspondence with the hypnogram of the spectral slope time-series are visually evident. (From Rosenblum, Jafarzadeh Esfahani, et al., 2025 with permission.)

The time-series of slope values were normalized by converting them into a series of z-scores per recording, then a 5th order Savitzky-Golay filter was applied with a frame length of 101. Next, a peak detection algorithm (Matlab's *findpeaks* function) was employed to find the local minima and maxima of the smoothed series, with 20 minute minimal distance between peaks and peak prominence of $|z| > 0.9$. Having detected the local extrema this way, fractal activity-based cycles were defined then as the period between two consecutive local maxima of the normalized and smoothed spectral slope series, see Figure 3.

3.2.4 Statistical analysis

Non-parametric tests were used as the normality assumption of the classical and fractal cycle durations did not hold according to the one-sample Kolmogorov-Smirnov test ($p < 0.05$). Spearman's correlations were assessed between the classical and fractal cycle durations for each dataset separately and for the pooled data as well.

The number of cycles detected by the two methods didn't always match, the mean number of the classical cycles was 4.7 ± 0.9, for the fractal cycles 4.6 ± 1.0 cycle per night, while the prevalence of cycle number mismatch was 34-55%, depending on dataset. In the cases where cycle numbers were equal between the two methods, the durations of the corresponding cycles were correlated. In case of cycle number difference between the methods, the cycle durations were averaged per participant and the average classical and fractal cycle durations were correlated.

Mann-Whitney U tests were used to make comparisons between the pediatric and young adult groups, MDD patients and controls, MDD patients with REM-suppressive versus REM-non-suppressive antidepressent treatments. Paired samples Wilcoxon test was applied to compare medicated and unmedicated states in MDD.

4 Results

4.1 Study 1 - Scale-free and oscillatory spectral measures of sleep stages in humans

4.1.1 Spectral slope

The spectral slope of the EEG showed a strong main effect of sleep stage, see Figure 4 [$F_{(4,824)} = 770.29, p < 10^{-5}, \eta_p^2 = 0.788$], with highest slope values (flattest PSDs) during wakefulness, then decreasing throughout non-REM sleep, reaching the lowest values (steepest spectral slopes) in slow wave (N3) sleep, and increased again in the REM stage. Age group also showed a significant main effect, revealing a general flattening of the EEG spectrum in sleep with the progression of age [$F_{(3,206)} = 6.47, p < 10^{-4}, \eta_p^2 = 0.086$]. A main effect of topography was observed [$F_{(4,824} = 113.33, p < 10^{-5}, \eta_p^2 = 0.355$] with decreased slope values in the more anterior EEG channels. Interaction effects were strongest in the case of stage-region [$F_{(16,3296)} = 55.23, p < 10^{-5}, \eta_p^2 = 0.211$] and stage-region-age [$F_{(48,32)} = 4.95, p < 10^{-5}, \eta_p^2 = 0.067$], see Figure 4, where flattening of the spectral slope in SWS with aging can be especially nicely noted, indicating the deterioration of sleep quality in older subjects.

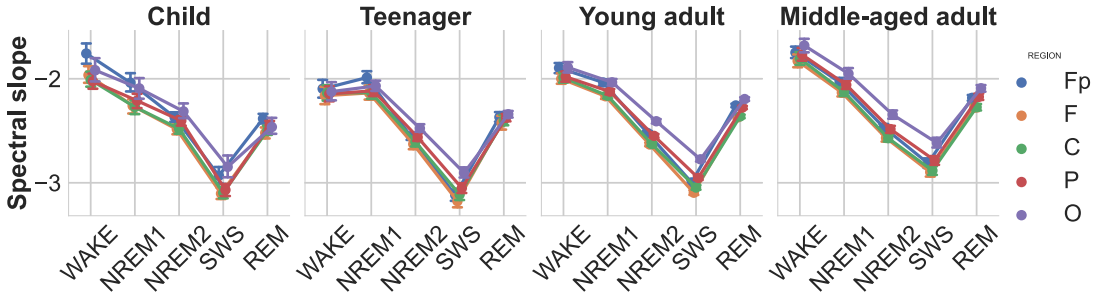

Figure 4: Spectral slopes as functions of sleep stage, brain region, and age group. Note the gradual decrease of slope values (decreasing spectral exponents, increasing steepness) during the course of deepening of NREM sleep, as well as a relatively increased slope in REM sleep (but still below the NREM1 values). Vertical bars denote 95% confidence intervals. (From Schneider et al., 2022.)

4.1.2 Spectral intercept

As intercept values provided by the FOOOF method were significantly correlated with the spectral slopes, the average Pearson's correlation coefficient was: $\langle r \rangle = 0.47$ (correlations between the spectral slope and intercept were calculated separately for each sleep stage and EEG channel, then Fisher-z transformed, averaged, and inverse

transformed). However, after adopting the alternative definition of the intercept as the power of the aperiodic component at the frequency of the dominant peak (Bódizs et al., 2021a) the correlation was eliminated, the average correlation reduced to $\langle r \rangle = -0.03$, thus statistical independence between the aperiodic parameters was ensured.

The main effect of sleep stage on the intercept parameter was still present [$F_{(4,836)} = 35.73, p < 10^{-5}, \eta_p^2 = 0.15$] with highest intercept values in SWS. The spectral intercept was increased in children in general (see Figure 5), contributing to the main effect of age [$F_{(3,209)} = 26.37, p < 10^{-4}, \eta_p^2 = 0.27$], in addition an interaction of sleep stage and brain region was also significant [$F_{(16,3344)} = 9.18, p < 10^{-5}, \eta_p^2 = 0.004$], with intercept increases more dominant in the frontopolar and frontal electrodes. There was a significant effect of sex on the spectral intercept [$F_{(1,13)} = 31.45$], showing increased values in women, a known general difference in EEG amplitudes, a result of skull-thickness dimorphism.

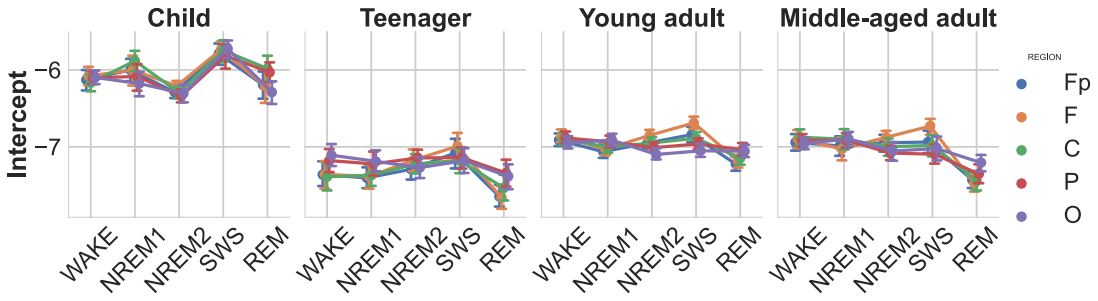

Figure 5: Modified spectral intercepts as functions of sleep stage, brain region, and age group. Note the particularly high intercepts in children, indicating high overall EEG amplitude values. Furthermore, the modified intercepts of SWS stage, especially the ones measured over the frontopolar recording regions, exceed other stages and regions. Vertical bars denote 95% confidence intervals. (From Schneider et al., 2022.)

4.1.3 Central peak frequency

Observing the central frequency of the dominant peak, a strong main effect of brain region was revealed [$F_{(4,824)} = 58.138, p < 10^{-5}, \eta_p^2 = 0.22$], with increased frequencies in the frontal and frontopolar derivations. Significant effects of age [$F_{(3,206)} = 17.2, p < 10^{-5}, \eta_p^2 = 0.2$] and sleep stage [$F_{(4,8)} = 15.584, p < 10^{-5}, \eta_p^2 = 0.07$] were found, the peak frequencies converging to sleep spindle frequencies in the non-REM stages, see Figure 6.

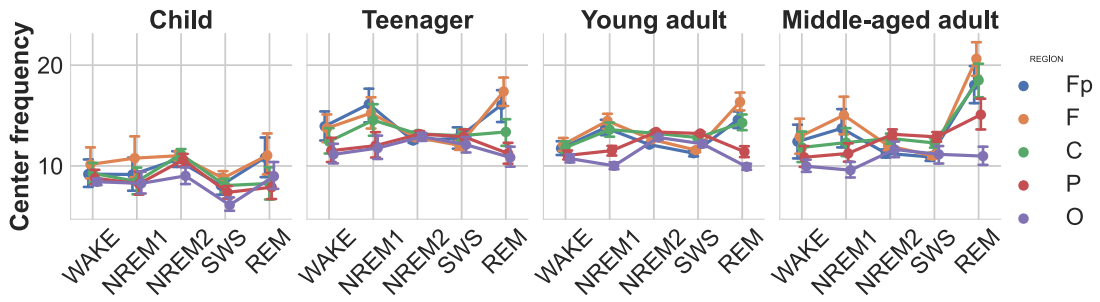

Figure 6: Central peak frequencies as functions of sleep stage, brain region, and age group. Note the high intersubject variability of central peak frequencies in WAKE, NREM1, and REM stages, as compared to NREM2 and SWS frequencies. This pattern indicates the presence of multiple oscillators with individually variable dominance in WAKE, NREM1, and REM stages, as well as a reliable dominance of sleep spindle waves (11–16 Hz) in NREM2 and SWS. Vertical bars denote 95% confidence intervals. (From Schneider et al., 2022.)

4.1.4 Peak power

The power of the dominant spectral peak also was significantly different between sleep stages $[F_{(4,824)} = 88.765, p < 10^{-5}, \eta_p^2 = 0.301]$ and brain regions $[F_{(4,824)} = 97.645, p < 10^{-5}, \eta_p^2 = 0.321]$. Some additional interaction effects were also revealed, for more details see supplemetary material of Schneider et al., 2022. It is worth to note the inverted U-shape of peak power with aging in NREM2 sleep, being most prominent in teenagers and young adults, yet diminished in children and middle-aged adults, see Figure 7.

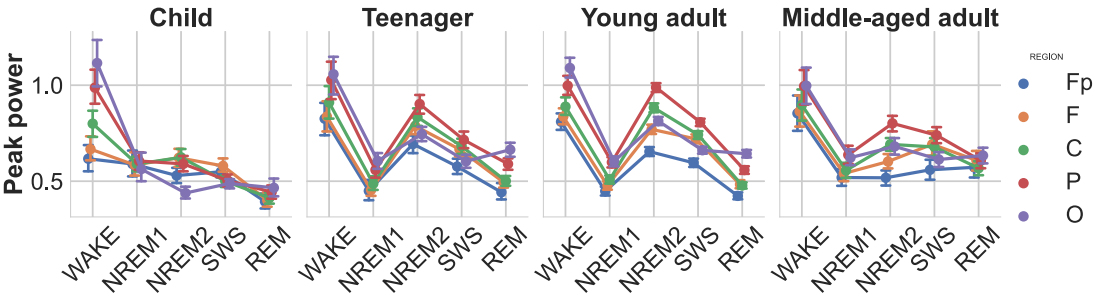

Figure 7: Power of the largest spectral peak as function of sleep stage, brain region, and age group. Note the high peak power in wakefulness and NREM2 sleep, known to be characterized by prominent alpha and sleep spindle oscillations, respectively. In addition, peak power is lower in children and in middle aged adults, as compared to teenagers and young adults. This pattern coheres with the ontogeny of sleep spindle oscillation in humans. Vertical bars denote 95% confidence intervals. (From Schneider et al., 2022.)

4.1.5 Adjusted spectral slope

It has been demonstrated that the parameters of the aperiodic spectral component of the EEG can be highly subject-specific (Demuru and Fraschini, 2020). In addition, we found that spectral slopes were significantly correlated between all sleep stages within subjects, the effect being more pronounced between subsequent sleep stages, see Figure 8. Assessing all possible pairings of (non-identical) sleep stages, correlation coefficients (Pearson's r) were in the range of $0.2 < r < 0.8$, mean $\langle r \rangle = 0.49$, with significances: $10^{-58} < p < 10^{-2}$.

In order to reduce the subject specificity of the spectral slope and increase the stage specificity, we propose a new measure termed the "adjusted spectral slope" that is defined as the deviation from the spectral slope measured during wakefulness before sleep in each individual. The index achieved this way indeed provided a slightly stronger sleep stage effect $[F_{(3,627)} = 1198.56, p < 10^{-5}, \eta_p^2 = 0.85]$, furthermore stage-region interaction $[F_{(12,2508)} = 62.99, p < 10^{-5}, \eta_p^2 = 0.23]$, see Figure 9.

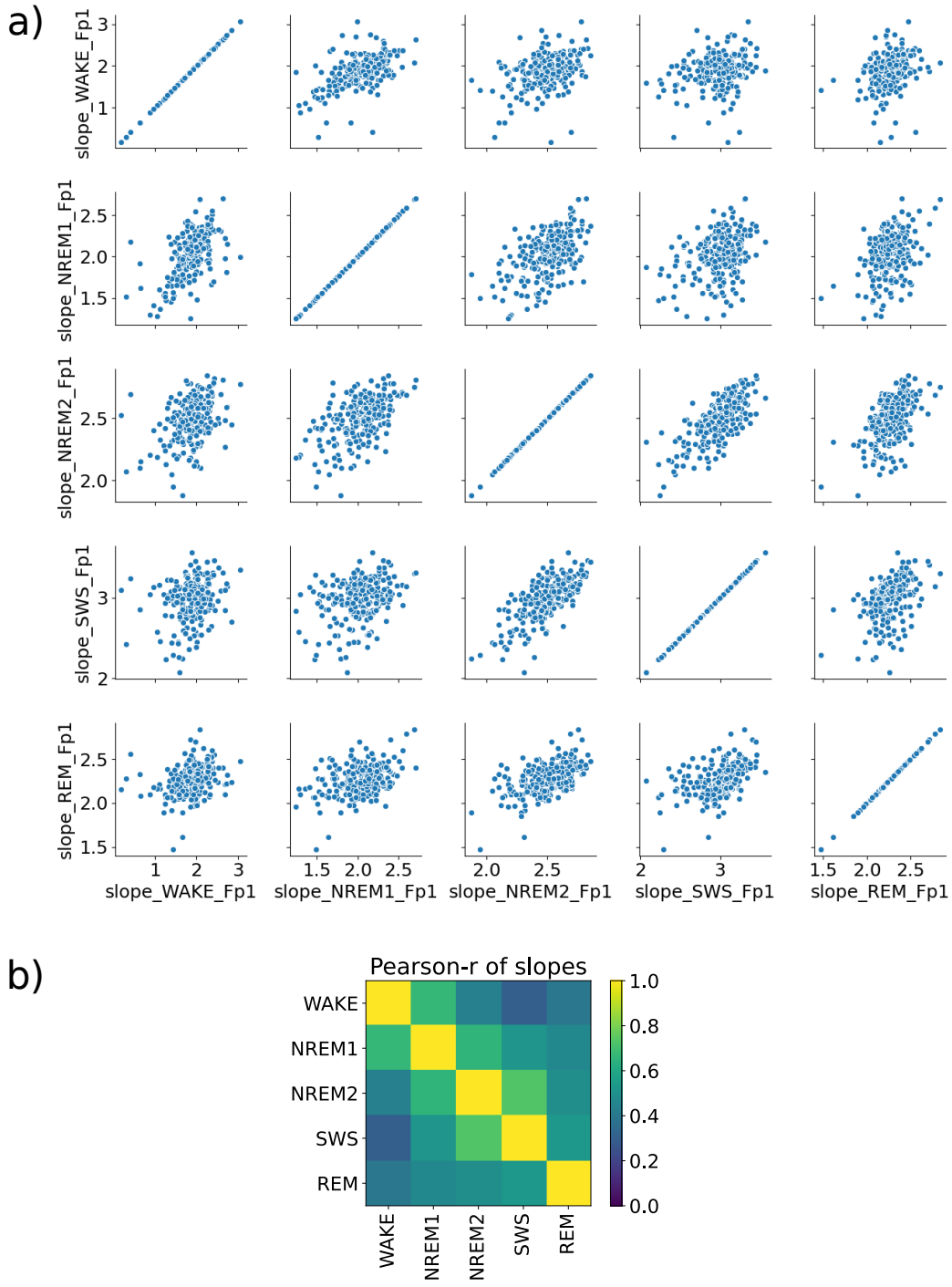

Figure 8: Correlation of spectral slopes between different sleep stages. a) Covariance plot of spectral slopes between different sleep stages, each point corresponding to a subject. b) Pearson correlations of spectral slopes between sleep stages in the case of the Fp1 channel. It can be noted that the values closer to the main diagonal are higher, suggesting that there is more correlation between subsequent sleep stages. (From supplementary material of Schneider et al., 2022.)

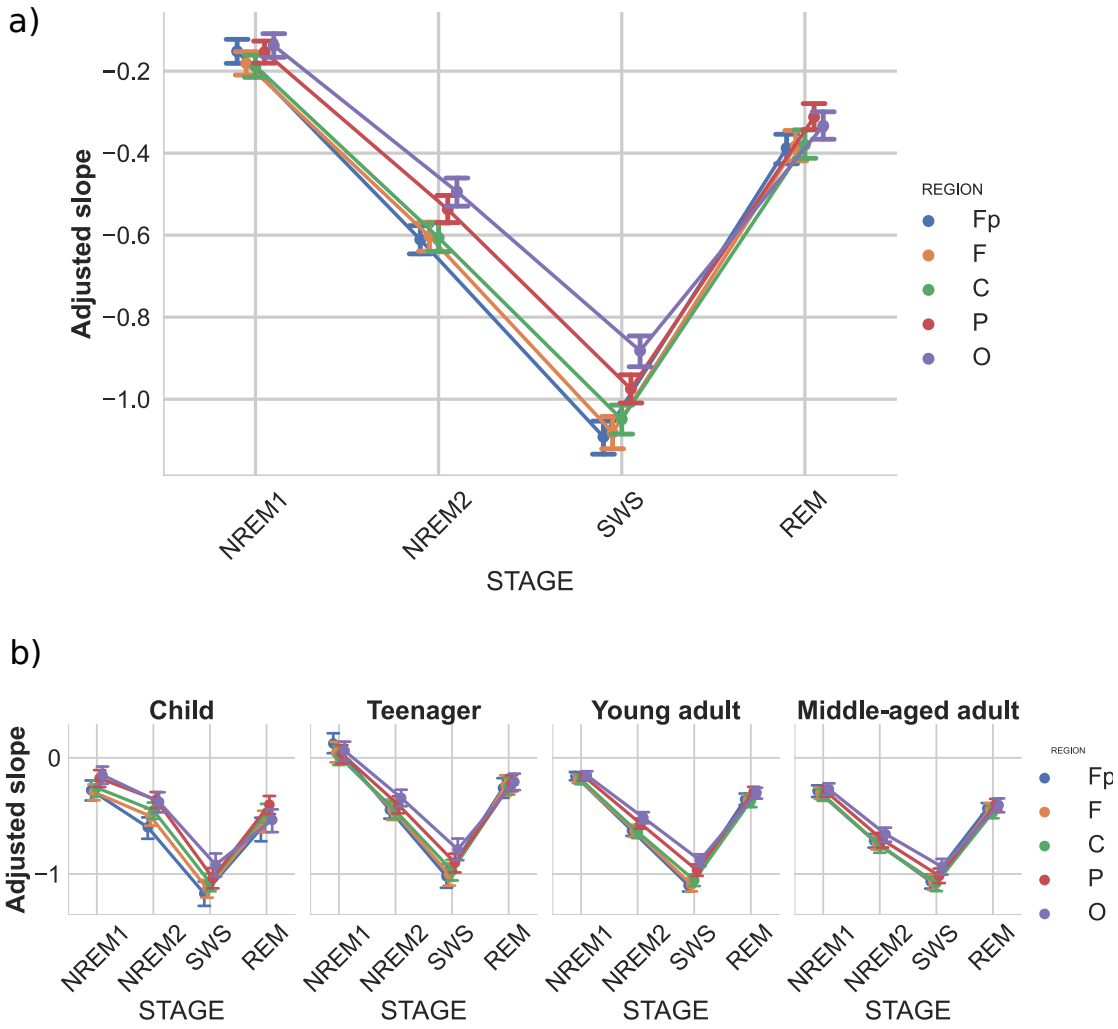

Figure 9: Adjusted spectral slopes as functions of sleep stage, brain region, and age group. Slopes were expressed as deviations from individual-, sleep stage-, and recording location-specific deviations from corresponding resting wakefulness values. a) Overall group mean, (b) age-group-specific means. Note the particularly reliable steepening of spectral slopes from NREM1 through NREM2 to SWS (indicated by decreasing slope values), as well as a considerable flattening in REM sleep, slightly above NREM2, but below NREM1-specific values. Vertical bars denote 95% confidence intervals. (From Schneider et al., 2022.)

4.2 Study 2 - Fractal cycles of sleep, a new aperiodic activity-based definition of sleep cycles

4.2.1 Fractal cycles in healthy adults

After visual inspection of overnight dynamics of the spectral slope of the EEG, it could be noted that the series usually peaks during REM episodes, and is locally minimal during non-REM sleep, see Figure 10A.

Furthermore, upon simple quantified inspection, known features of sleep were instantly revealed in the series. More specifically that the spectral slope alternated between peak-trough-peak 4-6 times during a night, and the duration of a cycle was around 90 minutes. The pooled average across cycles in all datasets of the fractal cycle duration was 89 ± 34 min, while for classical cycles 90 ± 25 min. Correlations between the per participant averaged durations of classical and fractal cycles were significant in all six datasets ($r = 0.4$–0.5), see Figure 10C and Table 2.

4.2.2 Correspondence between fractal and classical cycles

The 81% of fractal cycles could be matched with classical cycles upon visual inspection, 763 out of 940 cycles in all datasets, (and in 77-88% when datasets were analyzed separately). The number of fractal cycles matched classical cycles in 54% of all participants (111 out of 205), and the correlation of the durations of corresponding cycles was between $r = 0.5 - 0.8, p < 0.001$, see Table 2. In participants with fractal and classical cycle number mismatch, the average cycle number difference (fractal-classical) was -0.23 ± 1.23 cycles, ranged between -2 and 2, in these cases lower correlations were found between the cycle numbers ($r = 0.28, p = 0.006$) and cycle durations ($r = 0.278, p = 0.006$), see such an example in Figure 10B. It should be noted that despite the fact that the total number of cycles differ, some fractal cycle timings still matched the classical ones.

4.2.3 Fractal cycles in children

In the following, a child group (n=21, Dataset 6) in the age range of 8-17 years (mean: 12.4 ± 3.1 years) was compared to young adult participants selected from the rest of the datasets (n=24) in the age range of 23-25 years (mean: 24.8 ± 0.9 years), by the age at which the brain maturation process is supposedly complete.

Children manifested significantly shorter fractal cycle durations of 76 ± 34 min, while for young adults cycles were around 94 ± 32 min ($p < 0.001$, Cohen's d=-0.57), there was a similar difference in the classical cycles as well with 80 ± 23 min

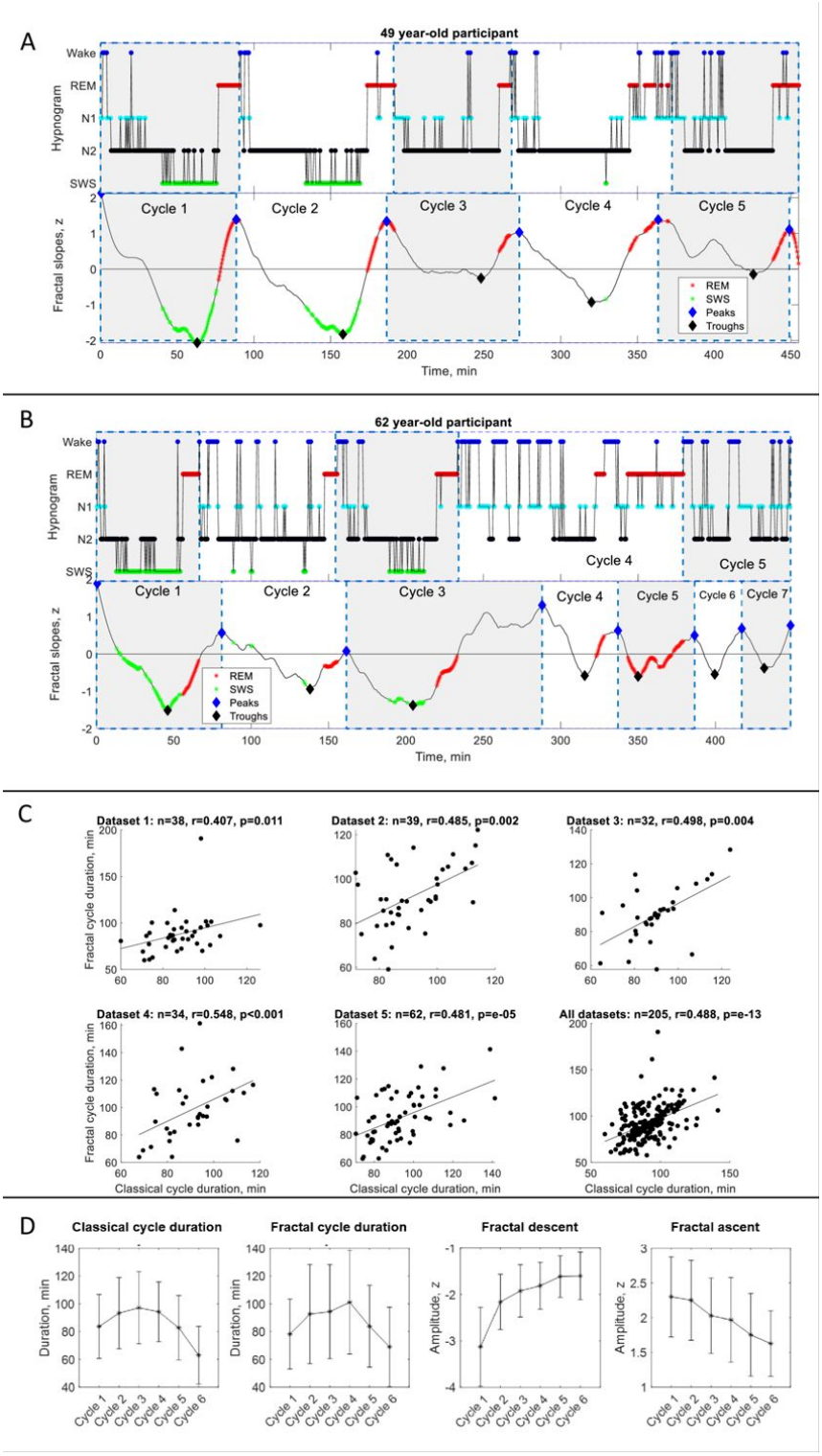

Figure 10: Fractal cycles in healthy adults, cycle turning points are the local maxima of the z-normalized and smoothed spectral slope series. Individual examples of **A)** matching and **B)** mismatching classical and fractal cycles. **C)** Correlation of average fractal and classical cycle durations per participant. **D)** Cycle-to-cycle dynamics of cycle durations, fractal descents and ascents (the amplitude difference from peak to through (and through to peak) within a cycle). (From Rosenblum, Jafarzadeh Esfahani, et al., 2025.)

	Dataset 1	Dataset 2	Dataset 3	Dataset 4	Dataset 5	Pooled dataset
Nr. of participants	38	39	32	34	62	205
TST [min]	394 ± 55	430 ± 26	434 ± 37	445 ± 62	467 ± 38	438 ± 51
Classical cycle duration [min]	86.2 ± 23.3	90.0 ± 21.3	89.0 ± 22.7	92.2 ± 23.7	91.9 ± 29.0	90.1 ± 24.9
Fractal cycle duration [min]	86.4 ± 35.2	90.0 ± 25.5	86.4 ± 31.2	94.7 ± 37.1	89.9 ± 37.1	89.1 ± 34.0
Classical-fractal cycles duration correlation, r	0.407	0.485	0.498	0.548	0.481	0.488
Classical-fractal cycles duration correlation, p	0.011	0.002	0.004	0.001	10^{-5}	10^{-13}
Match between classical and fractal cycles duration and timing, % cycles	78	88	82	87	77	81
Participants with all classical and fractal cycles matching % participants	53	62	66	53	45	54
Nr. of fractal cycles	167	171	152	152	298	940
Nr. of classical cycles	171	180	146	161	303	961

Table 2: Classical and fractal cycle descriptives of healthy adults. TST - total sleep time. (Adopted from Rosenblum, Jafarzadeh Esfahani, et al., 2025.)

in children and 90 ± 22 min in young adults ($p < 0.001$, Cohen's d=-0.42), see Figure 11C,D.

Using slightly more complex (ANCOVA) models separately for both cycle durations as the dependent, the group as the independent variable and age as a covariate, the differences were more pronounced in the fractal cycle durations ($F_{(1,43)} = 4.5$, $\eta_p^2 = 0.18$) between the two age groups, compared to differences in the classical cycle durations ($F_{(1,43)} = 3.1$, $\eta_p^2 = 0.13$).

When comparing the durations cycle-by-cycle overnight, a reduction in classical cycle duration was found only in the fourth cycle in children compared to young adults (Cohen's d=-1.0), while fractal cycle durations significantly differed between the two groups in the first two sleep cycles (Cohen's d=-0.61-0.72), see Figure 11E.

4.2.4 Age and fractal cycles

The effect of age on sleep cycle duration was also investigated in the pooled healthy adult dataset in the age range of 18-75 years (mean:33.5 years). A reduction of mean fractal cycle duration was associated with the progression of age (r=-0.19, $p = 0.006$), in order to rule out intra-sleep awakenings as a confounding factor the correlation between wake after sleep onset (WASO) and fractal cycle duration was assessed and found to be non-significant (r=0.01, $p = 0.969$). In addition, the relationship between fractal cycle duration and age was reevaluated in a partial correlation analysis, while controlling for WASO, which proved to be still significant (r=-0.16, $p = 0.011$).

Similarly, REM latency was also considered as a possible confounding factor, as it is know to be correlated with age. Nevertheless, the partial correlation between average fractal cycle duration and age was significant when adjusting for REM latency (r=-0.16, $p = 0.025$), however correlation between cycle duration and REM latency was not, when controlling for age (r=0, $p = 0.746$).

It should be noted, however, that the above effects were only significant for the pooled datasets and disappeared when including the dataset of children (Dataset 6). Furthermore in contrast to the findings in the fractal cycle durations, the average classical cycle duration didn't correlate with age in the pooled or in the separate datasets.

4.2.5 Fractal cycles in MDD

In order to evaluate the clinical applicability of the method, fractal cycle durations were compared between healthy controls and patients with major depressive disorder (MDD).

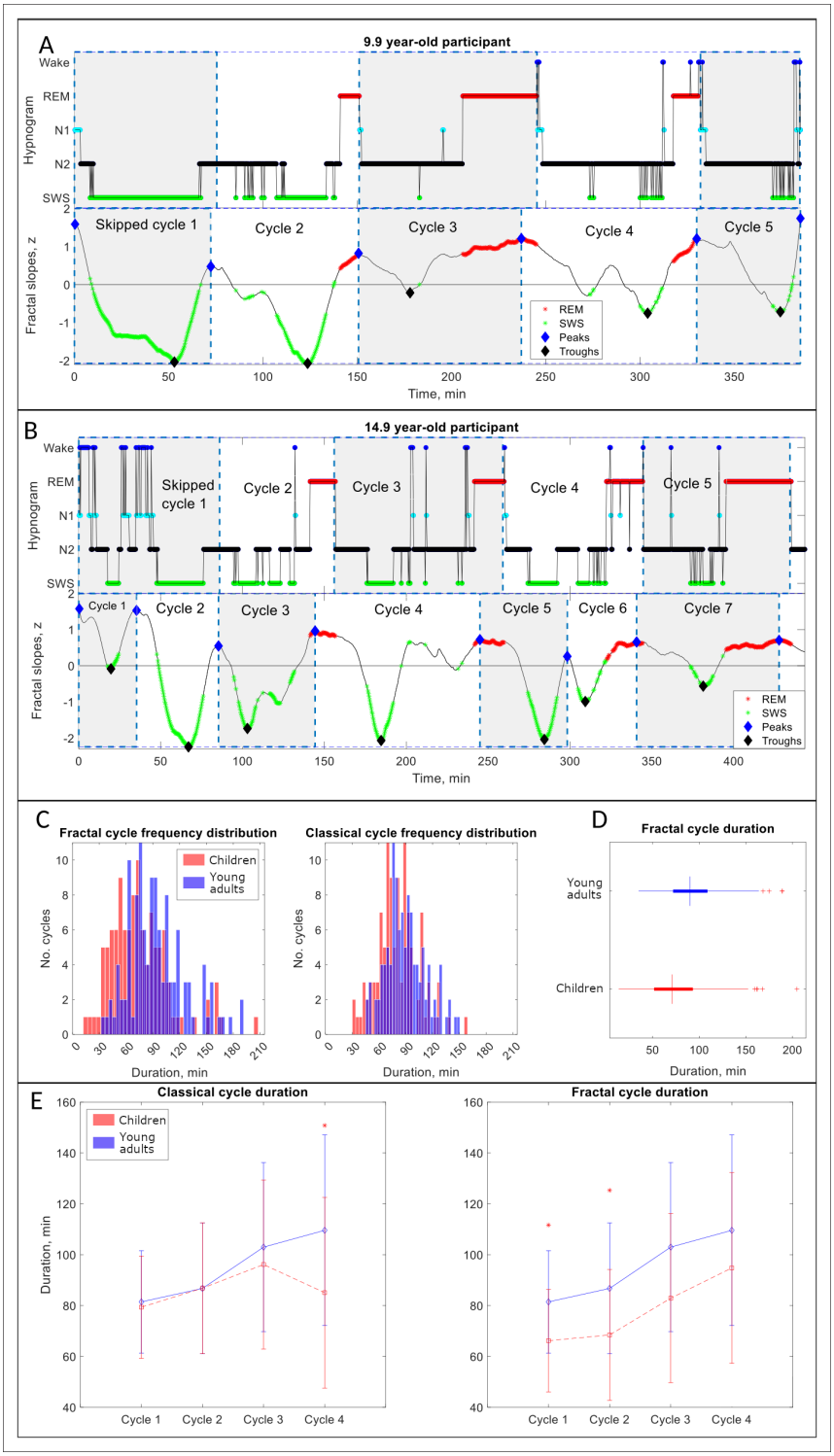

Figure 11: Comparison of fractal cycle duration between the age groups of children and young adults: **A)** classical (top) and fractal cycles (bottom) in a participant from the child group. **B)** comparison of classical (top) and fractal cycles (bottom) in a young adult participant. **C)** distributions of cycle durations with the two different methods (subplots) and age groups (colors). **D)** whisker plot of fractal cycle durations by age group. **E)** cycle-by-cycle comparison of age effects in the classical (left) and fractal cycle durations (right). (* marks a significant statistical difference between the groups.) (From Rosenblum, Jafarzadeh Esfahani, et al., 2025.)

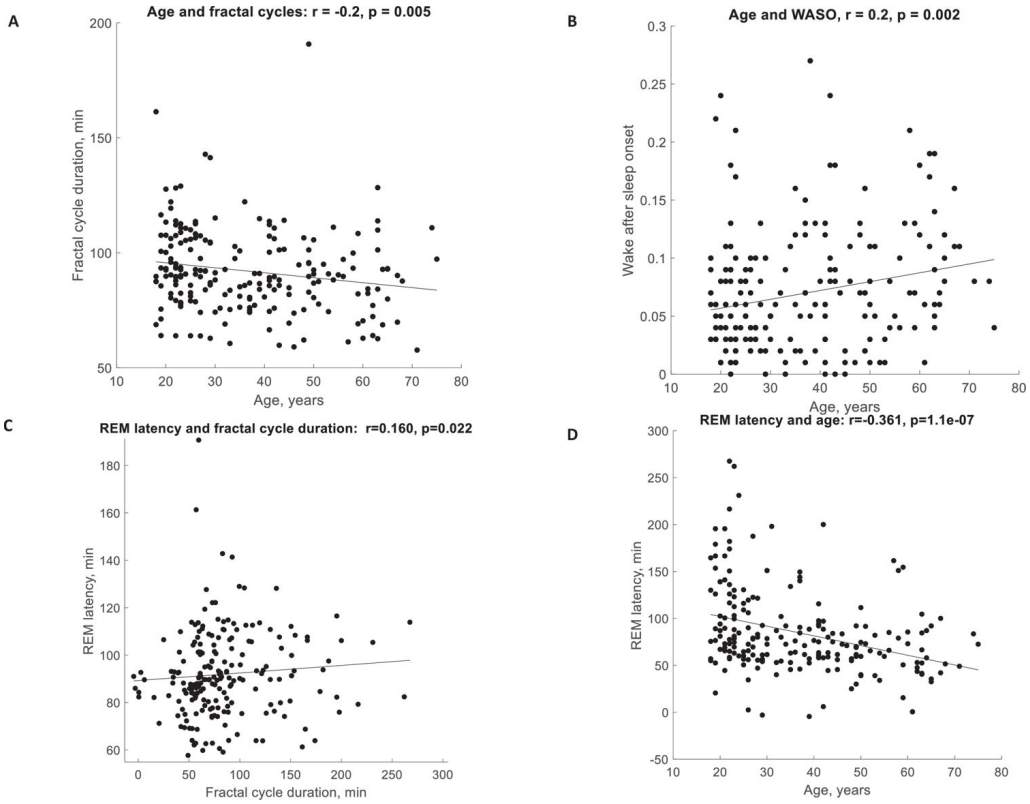

Figure 12: Associations between mean fractal cycle duration, age, wake after sleep onset (WASO) and REM latency. While both WASO and REM latency were significantly correlated with age, partial correlations remained significant between mean fractal cycle duration and age even after adjusting for these. (From Rosenblum, Jafarzadeh Esfahani, et al., 2025.)

Dataset	Group	N	Cycles	Duration [min]	p	d
1	HC	38	167	84 ± 35	-	-
	MDD, long-term med.	40	143	97 ± 43	0.001	0.3
2	HC	39	171	90 ± 26	-	-
	MDD, unmed.	38	155	92 ± 38	n.s.	-
	MDD, 7d med.	-	133	107 ± 51	0.0001	0.5
	REM-non-suppr.	17	63	95 ± 44	-	-
	REM-suppr.	21	70	121 ± 55	0.003	0.5
3	HC	32	154	88 ± 32	-	-
	MDD, 7d med.	33	122	107 ± 48	0.0001	0.5
	MDD, 28d med.	-	100	106 ± 51	0.001	0.4

Table 3: Fractal cycle statistics in healthy controls (HC) and patients with major depressive disorder (MDD) under different treatments. (Adopted from Rosenblum, Jafarzadeh Esfahani, et al., 2025.)

An increase in fractal cycle duration was found in both short- and long-term medicated MDD patients relative to controls. Dataset 1 included long-term medicated patients, their fractal cycle durations were significantly longer (97 ± 43 min) than those of healthy controls (84 ± 35 min, $p = 0.001$, Cohen's d=0.3). In Dataset 3 a significant slowing of fractal cycles was present after 7 days of medication (107 ± 48 min, $p < 0.001$, Cohen's d=0.5) and persisted after 28 days (106 ± 51 min, $p = 0.001$, Cohen's d=0.4) when compared to the baseline unmedicated states of the same individuals (88 ± 32 min), see Table 3 and Figure 13B.

In Dataset 2, it was also revealed that the type of antidepressant medication (REM-suppressive vs REM-non-suppressive) is also and important factor when comparing sleep cycles of MDD patients. Fractal cycles in patients taking REM-suppressants were significantly longer (95 ± 44 min, $p = 0.003$, Cohen's d=0.5) than in those under REM-non-suppressive treatment (121 ± 55 min). Differences between healthy controls and unmedicated MDD patients were non-significant, see Table 3.

When grouping all three datasets MDD patients under medication exhibited slower fractal sleep cycles (104 ± 49 min, $p < 0.001$) compared to controls (88 ± 31 min), see Figure 13C which effect was most prominent in the first sleep cycle (Figure 13D).

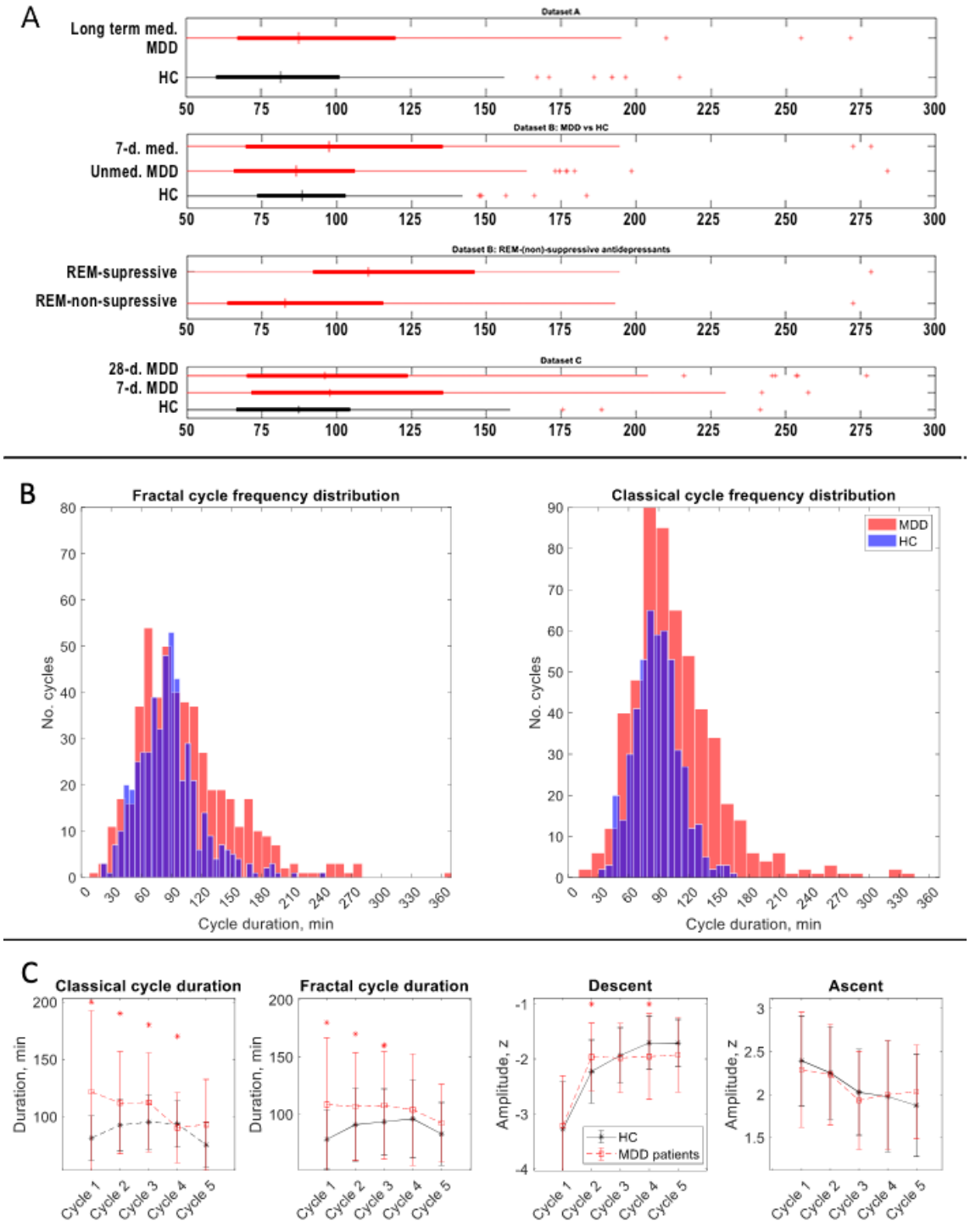

Figure 13: Comparison of classical and fractal cycles in healthy controls (HC) and major depressive disorder patients (MDD): **A)** under different medication statuses, **B)** pooled distributions of cycle durations by method and disorder group, **C)** overnight dynamics of cycle parameters by cyles. (* marks a significant statistical difference between the groups.) (From Rosenblum, Jafarzadeh Esfahani, et al., 2025.)

5 Discussion

Both above presented studies have demonstrated that the fractal component of the EEG carries meaningful information about sleep, and that the parametrization of the power-spectral density can provide a basis for a more objective assessment of sleep. In the following we discuss these findings in a wider context of the literature.

5.1 The spectral slope of EEG reflects sleep depth

The analyses in Study 1, have shown that most of the variance in the spectral slope can be explained by sleep stages, and that deeper sleep stages are reliably associated with more steep spectral slopes (more negative spectral exponents), with values around and slightly above -2 in wakefulness, then decreasing in NREM sleep until reaching the minimal value of -3 in SWS, and increased again in REM sleep to above -2.5.

Known effects of sleep deterioration associated with aging were also reflected in the fractal component, as there was a noticeable increase in the spectral slopes in older age groups in NREM2 and SWS sleep. In addition the recording region-dependency of the slope was also reproduced, with steeper spectra in more anterior electrodes (Voytek et al., 2015, Bódizs et al., 2021b, Pathania et al., 2022).

The observation that the fractal component of brain activity is distinct in wakefulness and sleep has been demonstrated before, for example the fractal exponent calculated via coarse graining spectral analysis was shown to differ between wake and sleep EEG (Pereda et al., 1998), or in studies exploring the fractality of EEG signals in sleep through the Hurst-exponent (Weiss et al., 2011), which is known to be correlated with the spectral exponent in fractional noises. It was also shown before that the spectral slope can differentiate between states of wake, sleep and anesthesia (Colombo et al., 2019, Lendner et al., 2020). Nevertheless, the methodical assessment of all spectral parameters on a large sample size with focus on sleep stage differences presented in Study 1 was a novelty. The importance of the spectral slope in the context of sleep and arousal is also demonstrated by the vast literature that studied it since.

It was shown that after sleep deprivation, under accumulated sleep pressure, the spectral slopes had been significantly steeper during the first four sleep cycles, backing the hypothesis that the spectral slope reflects objective sleep depth and sleep/wake homeostasis. Furthermore, that inter-individual differences were smaller when using the spectral slope compared to the traditional indicator of sleep depth, slow-wave activity (SWA). (G. Horváth et al., 2022, G. Horváth and Bódizs, 2025).

In another approach (Kozhemiako et al., 2022) the spectral slope had been considered in the gamma frequency range (35-45 Hz) and its reliability to differentiate between sleep stages confirmed on a very large sample (N=10255), here effects of age and sex were also revealed, furthermore the importance of EEG reference choice highlighted.

A systematic analysis of developmental effects on the fractal EEG component during wakefulness and sleep was made in Favaro et al., 2023 on a sample of 160 subjects, children and adolescents in the age range of 2-17 years. Fitting the power-law in the 1-20 Hz range it was evidenced that while the spectral slope is reduced as sleep deepens, similar to our findings in Study 1, their values are increased both in sleep and wakefulness along maturation. Moreover, both deep (N2, N3) and light (N1) sleep and wakefulness presented gradually more distinct spectral slopes with the progression of age, suggesting a differentiation of vigilance states with maturation.

Our results were also replicated by a study (Höhn et al., 2024) that compared the broadband (1-45 Hz) and the gamma band spectral slopes across sleep stages, emphasizing that the choice of the fitting frequency range is important. It was shown that while the broadband spectral slopes in REM were flatter and more similar to values of wakefulness, the gamma band slopes are steeper in this stage, making REM a heterogenous state in this perspective.

A more detailed analysis of aperiodic activity in REM sleep (Rosenblum, Bogdány, et al., 2025) revealed that the tonic and phasic REM states also show distinct spectral slope values. While phasic REM sleep is generally characterized by bursts of eye movement and a state of sensory detachment from the environment, phasic REM exhibits increased responsiveness to external stimuli and lowered arousal thresholds. Broadband (2-30 Hz) spectral slopes were steeper in the phasic state, while high-band (30-48 Hz) slopes were flatter, further suggesting the ability of the spectral slope to reflect arousal states.

5.2 Spectral slope dynamics track sleep cycles

As the spectral slope of the EEG proved to be a robust indicator of arousal and sleep stages, taking a further step, the overnight evolution of the spectral slope was utilized in Study 2 to track dynamical changes in sleep and to identify the basic building blocks of sleep structure: sleep cycles. The hypothesis that the alteration of NREM and REM stages would be also reflected as cyclicity in the spectral slope time-series was confirmed, furthermore by detecting local extrema of the series a above a threshold, a new definition of sleep cycles could be made automatically, a process that traditionally requires cumbersome manual scoring.

It was observed that the fractal cycle durations were significantly correlated with classical cycles determined by manually scored hypnograms in the healthy and MDD patients as well. Shorter fractal cycle durations were revealed in children and adolescents compared to adults, furthermore a negative correlation between fractal cycle duration and age in the healthy adult group. Overall 81% of the fractal cycles corresponded to classical cycles, moreover cycles with skipped REM stages could also be detected by the new method.

We would like to note however that fractal cycles are inherently different in some aspects, and are supposed to provide a data-driven alternative definition of sleep cycles. The first difference being that while classical cycles are based on a set of categorical values (discrete sleep stages assigned by a human scorer), fractal cycles utilize the continuous real-valued series of the fractal slopes, which is more information rich and objective. Furthermore, the delineation of cycles is not always straightforward based on the hypnogram, for example with interrupted or skipped REM sleep, in contrast fractal cycles offer a straightforward definition, based on the local maxima of the spectral slope in time. A second difference is that the turning-point of classical cycles is defined as the end of a REM period, in contrast, the turning-point of fractal cycles is defined at a local maximum of the spectral slope, which usually occurs during REM, as a consequence longer REM periods can cause mismatches between the fractal and classical cycles.

The practical effectiveness of the newly defined method has been analyzed so far, and while the study of underlying mechanisms is out of the scope of the study, some hypotheses regarding the functional significance of fractal cycles can be made, based on the literature.

In the framework of the reciprocal-interaction model (Pace-Schott and Hobson, 2002), the cyclic alternation of NREM and REM sleep is generated by a complex bidirectional interaction of REM-on and REM-off neurons located in the pons and modulated by several neurotransmitters, however the cyclical fluctuation of acetylcholine is considered to be responsible for the periodic reoccurrence of REM sleep (Hobson et al., 2000, Nir and Tononi, 2010), furthermore it was shown that in rats cholinergic stimulation was associated with flatter spectral slopes (Park and Weber, 2020). According to this, the local maxima of the spectral slope correspond to peaking cholinergic activation, while minima reflect dominant aminergic activity.

Alternatively, noradrenergic locus coeruleus (LC) neurons are proposed as modulators of the NREM-REM transition, more precisely that while periods of high LC activity promote arousal, low LC activation is necessary for entry into REM. In this view, the ascending branch of the fractal cycles correspond to periods of

low noradrenaline release, thus allowing the transition from NREM to REM sleep (Osorio-Forero et al., 2024).

According to the neuronal transition probability (NTP) model, spectral patterns of moving towards and away from deep sleep are a result of firing rate transitions in neurons that activate the brainstem. With the deepening of sleep, beta power decreases, delta power increases up to a saturation point, during which sigma reaches a maximal point, then the reverse happens when moving away from deep sleep (Merica and Fortune, 2011). In terms of the spectral slope high delta-beta ratio means a steeper slope, as such, descents in the slope time series correspond to the deepening of sleep, and vice-versa.

From a higher-level perspective sleep has two antagonistic aspects: sensory detachment from the environment during which the restorative functions of sleep take effect and transient restorations of arousal maintaining the monitoring of the environment (Simor et al., 2022). In this context, we hypothesize that steeper slopes reflect states of increased sensory detachment and restorative sleep, while flatter slopes mean increased levels of alertness necessary for external monitoring. Another duality of sleep can be formulated in terms of reactive and predictive homeostasis of sleep. As homeostasis in general is defined as the ability to maintain an optimal internal state of the organism in the face of external or internal perturbations. Reactive homeostatic processes are ones that aim to restore this optimal state after a change already occurred, while predictive homeostasis refers to processes that initiate compensation in advance for anticipated perturbations. In this framework the restorative functions of sleep that dominate the first part of the night are termed reactive homeostatic processes that are a response to previously accumulated sleep pressure. After the dissipation of sufficient sleep pressure, processes for the anticipation of wakefulness take over, including dreaming, which prepares the brain for future challenges, make predictions about future rewards and punishments, and identify pieces of new information (Simor et al., 2023). We propose that this is reflected in the fractal cycles as local minima of the spectral slope become shallower overnight.

5.3 Effect of major depressive disorder on fractal cycles

In the last part of Study 2 the fractal cycles method was applied to a sample of major depressive disorder (MDD) patients, including subsamples of unmedicated and medicated states with different types of antidepressants, REM-suppressants vs. REM-non-suppressants.

Sleep disturbances and abnormal sleep architecture are between the main symp-

toms of MDD, manifesting reduced periods of SWS, dysregulated REM sleep with early onset, increased duration and density. It is also important to note that the vast majority of antidepressant medications reduce sleep related symptoms, while suppressing the REM phase, delaying the onset and shortening the duration of REM sleep (Palagini et al., 2013).

In Study 2, no significant cycle legnth differences were observed between unmedicated MDD patients and healthy controls. An increase in fractal cycle duration was found in medicated states of MDD patients relative to their unmedicated states and to healthy controls, these differences being more pronounced in the first sleep cycles. The effect of medication type was also significant, REM-suppressive antidepressants significantly prolonged fractal cycle durations, while REM-non-suppressive medications didn't present any cycle duration alterations compared to unmedicated states. Given the definition of a fractal cycle that is the interval between two consecutive peaks of the spectral slope intercept, usually coinciding with REM stages, we conclude that most alterations in the cycle durations were present due to the suppression and delayed onset of REM phases caused by antidepressants. Alternatively, a general flattening of spectral slopes due to medication could also lead to the detection of longer cycles, as the peak detection threshold in the fractal cycles method had been established on a healthy population, thus fewer threshold crossings in a given time could lead to longer cycles (Rosenblum et al., 2023).

5.4 Oscillatory parameters of EEG spectra

Besides the spectral slope of aperiodic brain activity, neural oscillations were also investigated in Study 1 as spectral peaks. The most dominant peak was selected and described by the parameters of center frequency, power and bandwidth.

When considering the periodic component of sleep EEG, we expected to identify some of the well-known, state-specific oscillation frequencies in different sleep stages: alpha waves (8-12 Hz) in resting wakefulness, sleep spindle activity (11-16 Hz) in NREM sleep, theta (4-8 Hz) and beta (16-30 Hz) activity during REM sleep. We also attempted to test whether topographic differences were present in the spindle oscillatory peak frequencies, as anterior spindles tend to be faster than posterior ones. After initial testing, some readjustments in the control parameters of the FOOOF fitting methods were found necessary, as the standard parameters didn't make the separate resolution of two nearby peaks possible. After the correction, effects of sleep stage, recording region and age were evaluated.

Significant stage, region and interaction effects were found. Stable alpha frequencies were revealed in the child group, however, the activity of the subjects while

awake had not been controlled during the recording procedure, which could have been the source of the variability. Sleep stages NREM2 and SWS were dominated by sleep spindle frequencies, in addition antero-posterior differences were observed, corresponding to the topographic gradient of frequency in fast vs. slow sleep spindles. Despite REM sleep being most associated with theta activity, the dominant peaks after removing the aperiodic component were distributed over the beta range, with frequencies decreasing in the anterior-posterior direction. Increased beta activity in REM had been reported before, especially frontally in the tonic phase of the REM sleep (Simor et al., 2019, Jouny et al., 2000), during which alpha and mu rhythms (6-12 Hz) could also emerge, then get desynchronized in phasic REM, paralleling patterns of waking motor cortex activity during resting vs. voluntary movement execution (De Carli et al., 2016). When comparing the mean values and the spatial distribution of peak center frequencies in NREM1 and REM, some similarities can be recognized, which could be explained by the so-called *covert REM* hypothesis, according to which elements of REM sleep can appear during wake-sleep transition (Nielsen, 2000). Evidence had been found previously in support of the hypothesis, suggesting that spectral properties similar to REM sleep emerge in the EEG during the transition to sleep, more precisely after alpha dropout and before spindle activity (Bódizs et al., 2008).

Comparing the spectral powers of the dominant peaks across stages, wakefulness and NREM2 were most eminent, with lower powers in REM and NREM1 being similar in this respect as well. An interesting age effect was discovered in the peak power of the NREM2 stage, rising and waning over the as age increases, reaching its maximum in young adulthood. As pointed out before, peaks in NREM2 reflected sleep spindle activity, which is known to increase in amplitude from early childhood until maturation then decrease with the progression of age (Purcell et al., 2017).

6 Conclusions

Based on the results presented in the previous sections the following conclusions could be drawn:

- Aperiodic neural activity carries meaningful information about brain states in sleep, more precisely the spectral slope of the EEG is distinct in each sleep stage, thus a reliable indicator of objective sleep depth.
- As the overnight dynamics of the spectral slope reflected sleep architecture, it was possible to construct a mathematically formulated definition of sleep cycles based on the fractal activity.
- Fractal cycle length and timing coincided with manually annotated classical cycles in the majority of cases, furthermore it could detect cycles with of skipped or interrupted REM sleep.
- Known effects of aging on sleep were identified both in the aperiodic and oscillatory spectral parameters. Flattened spectral slopes reflected the shallowing of sleep with the progression of age, fractal cycle length increased in children and decreased in adults with age, peak power corresponding to spindle activity also followed an inverted U-curve, being maximal around the age of maturation.
- Having observed that fractal cycle durations were significantly increased in medicated patients with major depressive disorder, suggests the method could as a tool in the analysis of the effects of antidepressants on sleep, and potentially other clinical settings.

7 Summary

Besides neural oscillations manifested as spectral peaks in the power-spectral density (PSD) of the electroencephalogram (EEG), the brain constantly generates an aperiodic, fractal-like background activity that can be described by a power-law in the frequency domain. Several methods emerged recently that aim to separate the oscillatory and fractal components of electrophysiological signals and to give a parametric description at the same time.

In Study 1, we assessed how spectral parameters depended on sleep stages, age and brain region in a healthy population. Average PSDs were calculated for each sleep stage and EEG electrode per subject. Using the FOOOF method, the aperiodic and oscillatory spectral components were fitted and parameters of spectral slope and intercept, peak center frequency, peak power and peak bandwidth were extracted.

The spectral slope showed the most consistent and specific sensitivity to sleep stages, being the highest in wake and decreasing with the deepening of sleep, being minimal in slow-wave sleep, then increasing again in REM sleep. Significant effects and interactions with age and brain region were also revealed. Oscillatory parameters also showed sleep stage dependence, peak central frequencies being in the alpha band in wake, spindle range in NREM2 and SWS as expected, but some novel similarities were revealed between REM and NREM1 sleep, being dominated by beta activity after the removal of the aperiodic background. Furthermore, spindle peak power showed a non-linear effect, being lower in children and middle-aged adults, and most prominent in young adults.

In Study 2 the overnight dynamics of the slope reflected sleep structure, based on which a new definition of sleep cycles had been proposed. After smoothing and normalizing the slope time-series, local maxima were considered as markers of cycle turning points. The newly defined fractal cycles were compared to classical, manually annotated ones on datasets of healthy adults, children and major depressive disorder (MDD) patients, in most cases the cycles matching both in timing and duration. Fractal cycle durations showed significant effects of age, increasing in children and decreasing in healthy adults, even after controlling the possible confounding effects of wake after sleep onset and REM latency. Fractal cycle durations differed in medicated MDD patients from their own unmedicated state and healthy controls. The effect of medication was significant only for REM-suppressing antidepressants.

Overall, the parametric description of EEG spectra showed potential to serve as a basis for the objective characterization of sleep states, paving the way toward a data-driven, biologically plausible evaluation of human sleep, providing an alternative to rule-based, manual scoring, furthermore, suggesting clinical applicability.

8 References

Bédard, C., Kröger, H., & Destexhe, A. (2006). Does the 1 / f frequency scaling of brain signals reflect self-organized critical states? *Physical Review Letters*, *97*(11), 118102. https://doi.org/10.1103/PhysRevLett.97.118102

Beggs, J. M., & Plenz, D. (2003). Neuronal avalanches in neocortical circuits. *The Journal of Neuroscience*, *23*(35), 11167–11177. https://doi.org/10.1523/JNEUROSCI.23-35-11167.2003

Berry, R., Albertario, C. L., Harding, S., Uoyd, R. M., Plante, D. T., Quan, S. F., & Vaughn, B. V. (2018). The aasm manual for the scoring of sleep and associated events: Rules, terminology and technical specifications (version 2.) *American Academy of Sleep Medicine*.

Bódizs, R., Horváth, C. G., Szalárdy, O., Ujma, P. P., Simor, P., Gombos, F., Kovács, I., Genzel, L., & Dresler, M. (2022). Sleep-spindle frequency: Overnight dynamics, afternoon nap effects, and possible circadian modulation [_eprint: https://onlinelibrary.wiley.com/doi/pdf/10.1111/jsr.13514]. *Journal of Sleep Research*, *31*(3), e13514. https://doi.org/10.1111/jsr.13514

Bódizs, R., Schneider, B., Ujma, P. P., Horváth, C. G., Dresler, M., & Rosenblum, Y. (2024). Fundamentals of sleep regulation: Model and benchmark values for fractal and oscillatory neurodynamics. *Progress in Neurobiology*, *234*, 102589. https://doi.org/10.1016/j.pneurobio.2024.102589

Bódizs, R., Sverteczki, M., & Mészáros, E. (2008). Wakefulness–sleep transition: Emerging electroencephalographic similarities with the rapid eye movement phase. *Brain Research Bulletin*, *76*(1), 85–89. https://doi.org/10.1016/j.brainresbull.2007.11.013

Bódizs, R., Szalárdy, O., Horváth, C., Ujma, P. P., Gombos, F., Simor, P., Pótári, A., Zeising, M., Steiger, A., & Dresler, M. (2021a). A set of composite, non-redundant EEG measures of NREM sleep based on the power law scaling of the fourier spectrum. *Scientific Reports*, *11*(1). https://doi.org/10.1038/s41598-021-81230-7

Bódizs, R., Szalárdy, O., Horváth, C., Ujma, P. P., Gombos, F., Simor, P., Pótári, A., Zeising, M., Steiger, A., & Dresler, M. (2021b). A set of composite, non-redundant EEG measures of NREM sleep based on the power law scaling of the fourier spectrum [Publisher: Nature Publishing Group]. *Scientific Reports*, *11*(1), 2041. https://doi.org/10.1038/s41598-021-81230-7

Buzsáki, G. (2006, October 26). *Rhythms of the brain*. Oxford University Press. https://doi.org/10.1093/acprof:oso/9780195301069.001.0001

Colombo, M. A., Napolitani, M., Boly, M., Gosseries, O., Casarotto, S., Rosanova, M., Brichant, J.-F., Boveroux, P., Rex, S., Laureys, S., Massimini, M., Chieregato, A., & Sarasso, S. (2019). The spectral exponent of the resting EEG indexes the presence of consciousness during unresponsiveness induced by propofol, xenon, and ketamine. *NeuroImage*, *189*, 631–644. https://doi.org/10.1016/j.neuroimage.2019.01.024

De Carli, F., Proserpio, P., Morrone, E., Sartori, I., Ferrara, M., Gibbs, S. A., De Gennaro, L., Lo Russo, G., & Nobili, L. (2016). Activation of the motor cortex during phasic rapid eye movement sleep. *Annals of Neurology*, *79*(2), 326–330. https://doi.org/10.1002/ana.24556

Demuru, M., & Fraschini, M. (2020). Eeg fingerprinting: Subject-specific signature based on the aperiodic component of power spectrum. *Computers in Biology and Medicine*, *120*, 103748. https://doi.org/10.1016/j.compbiomed.2020.103748

Donoghue, T., Dominguez, J., & Voytek, B. (2020). Electrophysiological frequency band ratio measures conflate periodic and aperiodic neural activity [Publisher: Society for Neuroscience Section: Research Article: New Research]. *eNeuro*, *7*(6). https://doi.org/10.1523/ENEURO.0192-20.2020

Donoghue, T., Haller, M., Peterson, E. J., Varma, P., Sebastian, P., Gao, R., Noto, T., Lara, A. H., Wallis, J. D., Knight, R. T., Shestyuk, A., & Voytek, B. (2020). Parameterizing neural power spectra into periodic and aperiodic components. *Nature Neuroscience*, *23*(12), 1655–1665. https://doi.org/10.1038/s41593-020-00744-x

Dumermuth, L., & Molinari, L. (1987). Spectral analysis of eeg background activity. *Handbook of Electroencephalography and Clinical Neurophysiology: Methods of Analysis of Brain Electrical and Magnetic Signals*.

Favaro, J., Colombo, M. A., Mikulan, E., Sartori, S., Nosadini, M., Pelizza, M. F., Rosanova, M., Sarasso, S., Massimini, M., & Toldo, I. (2023). The maturation of aperiodic EEG activity across development reveals a progressive differentiation of wakefulness from sleep. *NeuroImage*, *277*, 120264. https://doi.org/10.1016/j.neuroimage.2023.120264

Feinberg, I., & Floyd, T. C. (1979). Systematic trends across the night in human sleep cycles. *Psychophysiology*, *16*(3), 283–291. https://doi.org/10.1111/j.1469-8986.1979.tb02991.x

Feinberg, I., March, J. D., Floyd, T. C., Fein, G., & Aminoff, M. J. (1984). Log amplitude is a linear function of log frequency in NREM sleep EEG of young

and elderly normal subjects. *Electroencephalography and Clinical Neurophysiology*, *58*(2), 158–160. https://doi.org/10.1016/0013-4694(84)90029-4

Freeman, W. J., & Zhai, J. (2008). Simulated power spectral density (psd) of background electrocorticogram (ecog). *Cognitive Neurodynamics*, *3*(1), 97–103. https://doi.org/10.1007/s11571-008-9064-y

G. Horváth, C., & Bódizs, R. (2025). Effect of sleep deprivation on fractal and oscillatory spectral measures of the sleep EEG: A window on basic regulatory processes. *NeuroImage*, *314*, 121260. https://doi.org/10.1016/j.neuroimage.2025.121260

G. Horváth, C., Szalárdy, O., Ujma, P. P., Simor, P., Gombos, F., Kovács, I., Dresler, M., & Bódizs, R. (2022). Overnight dynamics in scale-free and oscillatory spectral parameters of NREM sleep EEG [Publisher: Nature Publishing Group]. *Scientific Reports*, *12*(1), 18409. https://doi.org/10.1038/s41598-022-23033-y

Gao, R., Peterson, E. J., & Voytek, B. (2017). Inferring synaptic excitation/inhibition balance from field potentials. *NeuroImage*, *158*, 70–78. https://doi.org/10.1016/j.neuroimage.2017.06.078

Gerster, M., Waterstraat, G., Litvak, V., Lehnertz, K., Schnitzler, A., Florin, E., Curio, G., & Nikulin, V. (2022). Separating neural oscillations from aperiodic 1/f activity: Challenges and recommendations. *Neuroinformatics*, *20*(4), 991–1012. https://doi.org/10.1007/s12021-022-09581-8

He, B. J., Zempel, J. M., Snyder, A. Z., & Raichle, M. E. (2010). The temporal structures and functional significance of scale-free brain activity. *Neuron*, *66*(3), 353–369. https://doi.org/10.1016/j.neuron.2010.04.020

Hobson, J. A., Pace-Schott, E. F., & Stickgold, R. (2000). Dreaming and the brain: Toward a cognitive neuroscience of conscious states. *The Behavioral and Brain Sciences*, *23*(6), 793–842, discussion 904–1121. https://doi.org/10.1017/s0140525x00003976

Höhn, C., Hahn, M. A., Lendner, J. D., & Hoedlmoser, K. (2024). Spectral slope and lempel–ziv complexity as robust markers of brain states during sleep and wakefulness [Publisher: Society for Neuroscience Section: Research Article: New Research]. *eNeuro*, *11*(3). https://doi.org/10.1523/ENEURO.0259-23.2024

Jouny, C., Chapotot, F., & Merica, H. (2000). EEG spectral activity during paradoxical sleep: Further evidence for cognitive processing. *NeuroReport*, *11*(17), 3667–3671. https://doi.org/10.1097/00001756-200011270-00016

Kozhemiako, N., Mylonas, D., Pan, J. Q., Prerau, M. J., Redline, S., & Purcell, S. M. (2022). Sources of variation in the spectral slope of the sleep EEG [Publisher: Society for Neuroscience Section: Research Article: New Research]. *eNeuro*, *9*(5). https://doi.org/10.1523/ENEURO.0094-22.2022

Lendner, J. D., Helfrich, R. F., Mander, B. A., Romundstad, L., Lin, J. J., Walker, M. P., Larsson, P. G., & Knight, R. T. (2020). An electrophysiological marker of arousal level in humans. *eLife*, *9*. https://doi.org/10.7554/elife.55092

Mandelbrot, B. B., & Van Ness, J. W. (1968). Fractional brownian motions, fractional noises and applications [Publisher: Society for Industrial and Applied Mathematics]. *SIAM Review*, *10*(4), 422–437. https://doi.org/10.1137/1010093

Matthis, P., Scheffner, D., & Benninger, C. (1981). Spectral analysis of the EEG: Comparison of various spectral parameters. *Electroencephalography and Clinical Neurophysiology*, *52*(2), 218–221. https://doi.org/10.1016/0013-4694(81)90171-1

Merica, H., & Fortune, R. D. (2011). The neuronal transition probability (NTP) model for the dynamic progression of non-REM sleep EEG: The role of the suprachiasmatic nucleus (S. Yamazaki, Ed.). *PLoS ONE*, *6*(8), e23593. https://doi.org/10.1371/journal.pone.0023593

Miller, K. J., Sorensen, L. B., Ojemann, J. G., & Den Nijs, M. (2009). Power-law scaling in the brain surface electric potential (O. Sporns, Ed.). *PLoS Computational Biology*, *5*(12), e1000609. https://doi.org/10.1371/journal.pcbi.1000609

Milstein, J., Mormann, F., Fried, I., & Koch, C. (2009). Neuronal shot noise and brownian 1/f2 behavior in the local field potential [Publisher: Public Library of Science]. *PLOS ONE*, *4*(2), e4338. https://doi.org/10.1371/journal.pone.0004338

Nielsen, T. A. (2000). A review of mentation in REM and NREM sleep: "covert" REM sleep as a possible reconciliation of two opposing models. *Behavioral and Brain Sciences*, *23*(6), 851–866. https://doi.org/10.1017/S0140525X0000399X

Nir, Y., & Tononi, G. (2010). Dreaming and the brain: From phenomenology to neurophysiology. *Trends in Cognitive Sciences*, *14*(2), 88–100. https://doi.org/10.1016/j.tics.2009.12.001

Osorio-Forero, A., Foustoukos, G., Cardis, R., Cherrad, N., Devenoges, C., Fernandez, L. M. J., & Lüthi, A. (2024, March 7). Noradrenergic locus coeruleus activity functionally partitions NREM sleep to gatekeep the NREM-REM

sleep cycle [Pages: 2023.05.20.541586 Section: New Results]. https://doi.org/10.1101/2023.05.20.541586

Pace-Schott, E. F., & Hobson, J. A. (2002). The neurobiology of sleep: Genetics, cellular physiology and subcortical networks. *Nature Reviews Neuroscience*, *3*(8), 591–605. https://doi.org/10.1038/nrn895

Palagini, L., Baglioni, C., Ciapparelli, A., Gemignani, A., & Riemann, D. (2013). REM sleep dysregulation in depression: State of the art. *Sleep Medicine Reviews*, *17*(5), 377–390. https://doi.org/10.1016/j.smrv.2012.11.001

Pani, S. M., Fraschini, M., Figorilli, M., Tamburrino, L., Ferri, R., & Puligheddu, M. (2021). Sleep-related hypermotor epilepsy and non-rapid eye movement parasomnias: Differences in the periodic and aperiodic component of the electroencephalographic power spectra. *Journal of Sleep Research*, *30*(5), e13339. https://doi.org/10.1111/jsr.13339

Park, S.-H., & Weber, F. (2020). Neural and homeostatic regulation of REM sleep. *Frontiers in Psychology*, *11*, 1662. https://doi.org/10.3389/fpsyg.2020.01662

Pathania, A., Euler, M. J., Clark, M., Cowan, R. L., Duff, K., & Lohse, K. R. (2022). Resting EEG spectral slopes are associated with age-related differences in information processing speed. *Biological Psychology*, *168*, 108261. https://doi.org/10.1016/j.biopsycho.2022.108261

Pereda, E., Gamundi, A., Rial, R., & González, J. (1998). Non-linear behaviour of human eeg: Fractal exponent versus correlation dimension in awake and sleep stages. *Neuroscience Letters*, *250*(2), 91–94. https://doi.org/10.1016/s0304-3940(98)00435-2

Peterson, E. J., Rosen, B. Q., Belger, A., Voytek, B., & Campbell, A. M. (2023). Aperiodic neural activity is a better predictor of schizophrenia than neural oscillations [Publisher: SAGE Publications Inc]. *Clinical EEG and Neuroscience*, *54*(4), 434–445. https://doi.org/10.1177/15500594231165589

Pritchard, W. S. (1992). The brain in fractal time: 1/f-like power spectrum scaling of the human electroencephalogram. *International Journal of Neuroscience*, *66*(1), 119–129. https://doi.org/10.3109/00207459208999796

Purcell, S. M., Manoach, D. S., Demanuele, C., Cade, B. E., Mariani, S., Cox, R., Panagiotaropoulou, G., Saxena, R., Pan, J. Q., Smoller, J. W., Redline, S., & Stickgold, R. (2017). Characterizing sleep spindles in 11,630 individuals from the national sleep research resource [Publisher: Nature Publishing Group]. *Nature Communications*, *8*(1), 15930. https://doi.org/10.1038/ncomms15930

Rechtschaffen A, K. A. (1968). *A manual of standardized terminology, techniques and scoring system of sleep stages in human subjects*. Los Angeles: Brain Information Service/Brain Research Institute, University of California.

Robertson, M. M., Furlong, S., Voytek, B., Donoghue, T., Boettiger, C. A., & Sheridan, M. A. (2019). EEG power spectral slope differs by ADHD status and stimulant medication exposure in early childhood. *Journal of Neurophysiology*, *122*(6), 2427–2437. https://doi.org/10.1152/jn.00388.2019

Rosenblum, Y., Bogdány, T., Nádasy, L. B., Chen, X., Kovács, I., Gombos, F., Ujma, P., Bódizs, R., Adelhöfer, N., Simor, P., & Dresler, M. (2025). Aperiodic neural activity distinguishes between phasic and tonic REM sleep [_eprint: https://onlinelibrary.wiley.com/doi/pdf/10.1111/jsr.14439]. *Journal of Sleep Research*, *34*(4), e14439. https://doi.org/10.1111/jsr.14439

Rosenblum, Y., Bovy, L., Weber, F. D., Steiger, A., Zeising, M., & Dresler, M. (2023). Increased aperiodic neural activity during sleep in major depressive disorder. *Biological Psychiatry Global Open Science*, *3*(4), 1021–1029. https://doi.org/10.1016/j.bpsgos.2022.10.001

Rosenblum, Y., Jafarzadeh Esfahani, M., Adelhöfer, N., Zerr, P., Furrer, M., Huber, R., Roest, F. F., Steiger, A., Zeising, M., Horváth, C. G., Schneider, B., Bódizs, R., & Dresler, M. (2025). Fractal cycles of sleep, a new aperiodic activity-based definition of sleep cycles (A. Peyrache & C. Büchel, Eds.) [Publisher: eLife Sciences Publications, Ltd]. *eLife*, *13*, RP96784. https://doi.org/10.7554/eLife.96784

Schneider, B., Szalárdy, O., Ujma, P. P., Simor, P., Gombos, F., Kovács, I., Dresler, M., & Bódizs, R. (2022). Scale-free and oscillatory spectral measures of sleep stages in humans [Publisher: Frontiers]. *Frontiers in Neuroinformatics*, *16*. https://doi.org/10.3389/fninf.2022.989262

Simor, P., Bogdány, T., & Peigneux, P. (2022). Predictive coding, multisensory integration, and attentional control: A multicomponent framework for lucid dreaming [Publisher: Proceedings of the National Academy of Sciences]. *Proceedings of the National Academy of Sciences*, *119*(44), e2123418119. https://doi.org/10.1073/pnas.2123418119

Simor, P., Peigneux, P., & Bódizs, R. (2023). Sleep and dreaming in the light of reactive and predictive homeostasis. *Neuroscience & Biobehavioral Reviews*, *147*, 105104. https://doi.org/10.1016/j.neubiorev.2023.105104

Simor, P., Van Der Wijk, G., Gombos, F., & Kovács, I. (2019). The paradox of rapid eye movement sleep in the light of oscillatory activity and cortical syn-

chronization during phasic and tonic microstates. *NeuroImage*, *202*, 116066. https://doi.org/10.1016/j.neuroimage.2019.116066

Sörnmo, L., & Laguna, P. (2005). *Bioelectrical signal processing in cardiac and neurological applications*. Elsevier. https://doi.org/10.1016/B978-0-12-437552-9.X5000-4

Ujma, P. P., Konrad, B. N., Gombos, F., Simor, P., Pótári, A., Genzel, L., Pawlowski, M., Steiger, A., Bódizs, R., & Dresler, M. (2017). The sleep EEG spectrum is a sexually dimorphic marker of general intelligence [Publisher: Nature Publishing Group]. *Scientific Reports*, *7*(1), 18070. https://doi.org/10.1038/s41598-017-18124-0

Voytek, B., Kramer, M. A., Case, J., Lepage, K. Q., Tempesta, Z. R., Knight, R. T., & Gazzaley, A. (2015). Age-related changes in 1/f neural electrophysiological noise [Publisher: Society for Neuroscience Section: Articles]. *Journal of Neuroscience*, *35*(38), 13257–13265. https://doi.org/10.1523/JNEUROSCI.2332-14.2015

Weiss, B., Clemens, Z., Bódizs, R., & Halász, P. (2011). Comparison of fractal and power spectral EEG features: Effects of topography and sleep stages. *Brain Research Bulletin*, *84*(6), 359–375. https://doi.org/10.1016/j.brainresbull.2010.12.005

Wen, H., & Liu, Z. (2016). Separating fractal and oscillatory components in the power spectrum of neurophysiological signal. *Brain topography*, *29*(1), 13–26. https://doi.org/10.1007/s10548-015-0448-0

Zempel, J. M., Politte, D. G., Kelsey, M., Verner, R., Nolan, T. S., Babajani-Feremi, A., Prior, F., & Larson-Prior, L. J. (2012). Characterization of scale-free properties of human electrocorticography in awake and slow wave sleep states [Publisher: Frontiers]. *Frontiers in Neurology*, *3*. https://doi.org/10.3389/fneur.2012.00076

9 Bibliography of the candidate

9.1 Publications of the thesis

Rosenblum, Y., Jafarzadeh Esfahani, M., Adelhöfer, N., Zerr, P., Furrer, M., Huber, R., Roest, F. F., Steiger, A., Zeising, M., Horváth, C. G., **Schneider, Bence**, Bódizs, R., & Dresler, M. (2025). Fractal cycles of sleep, a new aperiodic activity-based definition of sleep cycles (A. Peyrache & C. Büchel, Eds.) [Publisher: eLife Sciences Publications, Ltd]. *eLife,* ***IF: N/A***, *13*, RP96784. https://doi.org/10.7554/eLife.96784

Schneider, Bence, Szalárdy, O., Ujma, P. P., Simor, P., Gombos, F., Kovács, I., Dresler, M., & Bódizs, R. (2022). Scale-free and oscillatory spectral measures of sleep stages in humans [Publisher: Frontiers]. *Frontiers in Neuroinformatics,* ***IF: 3.5***, *16*. https://doi.org/10.3389/fninf.2022.989262

9.2 Other publications

Bódizs, R., **Schneider, Bence**, Ujma, P. P., Horváth, C. G., Dresler, M., & Rosenblum, Y. (2024). Fundamentals of sleep regulation: Model and benchmark values for fractal and oscillatory neurodynamics. *Progress in Neurobiology,* ***IF: 6.1***, *234*, 102589. https://doi.org/10.1016/j.pneurobio.2024.102589

G. Horváth, C., **Schneider, Bence**, Rozner, B., Koczur, M., & Bódizs, R. (2025). Interrelationships between sleep quality, circadian phase and rapid eye movement sleep: Deriving chronotype from sleep architecture. *Behavior Research Methods,* ***IF: 3.9***, *57*(5), 150. https://doi.org/10.3758/s13428-025-02671-w

Sándor, B., **Schneider, Bence**, Lázár, Z. I., & Ercsey-Ravasz, M. (2021). A novel measure inspired by lyapunov exponents for the characterization of dynamics in state-transition networks. *Entropy,* ***IF: 2.738***, *23*(1), 103. https://doi.org/10.3390/e23010103

Schneider, Bence, Dresler, M., Gombos, F., Kovács, I., & Bódizs, R. (2025, November 3). A broken power-law model of heart rate variability spectra in sleep. https://doi.org/10.1101/2025.11.01.685631

Schneider, Bence, Gombos, F., Kovács, I., & Bódizs, R. (2025, November 3). Spectral features of heart rate variability in williams syndrome during sleep. https://doi.org/10.1101/2025.11.01.685999

$\sum IF = 16.238$

10 Acknowledgments

First, I would like to thank my advisor, Róbert Bódizs, for his excellent professional guidance and openness during my doctoral work, which has granted me access and deep insights into this exciting scientific field.

Second, I am grateful to Yevgenia Rosenblum and Martin Dresler for their collaboration and for the experience to work in an international lab. Special thanks to Pál Czobor for his thorough review and insightful comments on the dissertation. I would also like to thank my colleague, Csenge G. Horváth, for her continuous help and valuable discussions, furthermore to the whole Sleep and Chronobiology Research Group.

Last, but not least, I would like to thank Zoltán Kozma and the rest of my family and friends for their support and encouragement.